Title
Unintended environmental impacts of nighttime freight logistics activities

Authors
Sathaye, Nakul
Harley, Robert
Madanat, Samer

Publication Date
2009-10-01

Unintended environmental impacts of nighttime freight logistics activities

Nakul Sathaye, Robert Harley, and Samer Madanat

WORKING PAPER
UCB-ITS-VWP-2009-11

UC Berkeley Center for Future Urban Transport
A VOLVO Center of Excellence

October 2009

Contents

Table of Figures

Table of Tables

Table of Acronyms and Symbols

ABL	Atmospheric Boundary Layer
BAAQMD	Bay Area Air Quality Management District
CalTrans	California Department of Transportation
CARB	California Air Resources Board
CO_2	Carbon Dioxide
EPA	U.S. Environmental Protection Agency
FD	Fundamental Diagram
G	Gram
Hr	Hour
I-x	Interstate Highway x, where x is a number
M	Meter
MFD	Macroscopic Fundamental Diagram
O_3	Ozone
PeMS	Freeway Performance Measurement System
$PM_{2.5}$	Particulate Matter with Diameter < 2.5 micrometers
pmf	Probability Mass Function
S	Second
VOC	Volatile Organic Compound

Abstract:

In recent years, the reduction of freight vehicle trips during peak hours has been a common policy goal. To this end, policies have been implemented to shift logistics operations to nighttime hours. The purpose of such policies has generally been to mitigate congestion and environmental impacts. However, the atmospheric boundary layer is generally more stable during the night than the day. Consequently, shifting logistics operations to the night may increase 24-hour average concentrations of diesel exhaust pollutants in many locations. This paper presents realistic scenarios for two California cities, which provide exhaust concentration and human intake estimates after temporal redistributions of daily logistics operations. Estimates are made for multiple redistribution patterns, including from 07:00-19:00 to 19:00-0:700, similar to daytime congestion charging polices and from 03:00-18:00 to 18:00-03:00, corresponding to the PierPASS program at the ports of Los Angeles and Long Beach. Results for these two redistribution scenarios indicate that 24-hour average exhaust concentrations would increase at most locations in California, and daily human intake is likely to worsen or be unimproved at best. These results are shown to be worse for inland than coastal settings, due to differences in meteorology. Traffic congestion effects are accounted for, using a new graphical method, which depicts how off-peak policies can be environmentally improving or damaging, depending on traffic speeds and meteorology. An investigation into the decreasing marginal environmental benefits of off-policies is then provided, through the application of traffic flow theory. Finally, related environmental and human exposure concerns are considered to provide a comprehensive policy discussion of the environmental effects of shifting logistics operations from day to night.

Keywords: City Logistics, Off-Peak, Nighttime Operations, Truck Traffic, Freight Policy, Atmospheric Dispersion

1. Introduction

Policies for shifting freight logistics operations away from highly impacting times and locations are receiving increased attention from policy makers and analysts (Eliasson et al., 2009; Giuliano and O'Brien, 2007; Hensher and Puckett, 2007; Holguin-Veras and Cetin, 2009; Holguin-Veras et al., 2006; Olszewski and Xie, 2005; Quak and de Koster, 2009; Sathaye et al., 2006). Such policies are not new, as records indicate their implementation as early as 2000 years ago (Holguin-Veras, 2008). Despite the important drawback of increased noise near residences, presently, the policy of shifting logistics operations to the night is becoming more widely accepted and promoted. The conventional wisdom is that off-peak policies are beneficial for transportation systems and the environment[1].

Off-peak policies are being implemented to induce more efficient utilization of transportation infrastructure in many locations around the world. For instance, nighttime delivery programs have been implemented with much success in many European cities (Geroliminis and Daganzo, 2005). A delivery program in Barcelona shows that logistics operations can be conducted at night without creating a detrimental noise problem (Forkert and Eichhorn, 2008). This city has also devoted lanes of some of its main boulevards to delivery operations during off-peak hours (Dablanc, 2007). The Port Authority of New York has also implemented a time of day pricing initiative to incentive off-peak operations (Holguin-Veras et al., 2006). In addition, consideration for off-peak policies is not limited to the urban scale. The passage of state legislation in California encourages port terminals to extend service hours to nights and weekends (Giuliano and O'Brien, 2007).

These implementations are generally supported by studies which indicate that off-peak policies, and especially shifts to night, can reduce traffic congestion and emissions (Browne et al., 2006; McKinnon, 2003; OECD, 2003). However, some previous studies have found that environmental impacts may

[1] Although noise is an important concern, the term environment will not account for noise in this paper.

increase. For example, in Southern California it has been shown that emissions can increase due to the circumvention of peak-period truck restrictions by the use of smaller vehicles (Campbell, 1995). Research on logistics in the Netherlands indicates that restrictions by time windows and vehicle type can increase emissions associated with deliveries (Quak and de Koster, 2009). Two previous studies use concepts of atmospheric science, which will be a focus of this paper, to show that exhaust concentrations can increase as a result of off-peak operations. One study provides estimates of the change in pollutant concentrations resulting from trucks, pointing out the potential problems resulting from off-peak policies (Panis and Beckx, 2007). An experimental study in southern California shows that pollutant concentrations, resulting from aggregate traffic, can be higher during pre-sunrise than daylight hours, despite lower total traffic levels (Hu et al., 2009). Such analyses have taken steps towards investigating the environmental impacts of off-peak policies, which are becoming increasingly important as the detrimental health impacts of diesel exhaust have become apparent (U.S. Environmental Protection Agency, 2002). However, current analyses of off-peak policies still generally neglect to incorporate a comprehensive assessment of environmental impacts.

A complete environmental assessment of city-logistics policies would involve the following steps:

1. Assessment of feasibility based on economic, political, administrative and social considerations

2. Assessment of adaptations by logistics operators

3. Assessment of the effects on traffic congestion

4. Assessment of the effects on tailpipe emissions from passenger and freight logistics vehicles (and possibly life-cycle emissions)

5. Assessment of resulting pollutant concentrations through atmospheric modeling

6. Estimation of environmental impacts (e.g. human intake)

Adjustments can be made to this general framework such as iterative prediction of logistics adaptations and traffic congestion. However, the general framework is valid for almost any city logistics policy. Many studies, including those mentioned above, focus on the first three steps, with a fair number considering the tailpipe emissions component of the fourth (Campbell, 1995; Giuliano and O'Brien, 2007; Quak and de Koster, 2007; Quak and de Koster, 2009). We additionally note the possibility that life-cycle emissions may be sensitive to certain policies (Facanha and Horvath, 2006; Sathaye et al., 2009). Although the fifth and sixth steps are often neglected, some studies do focus on making detailed impact assessments (Kinney et al., 2000; Wu et al., 2009). However, generalized values for monetary impact per emissions are more commonly used in policy analyses (Holguin-Veras and Cetin, 2009; Janic, 2007; Ubillos, 2008). Analysis approaches which account for only specific assessment steps or which use generalized values can be useful for deriving some insights, however results can be misleading due to the spatial and temporal variation of environmental impacts and the subtleties of transportation systems. Therefore, significant questions can remain about the usefulness and accuracy of these conclusions.

In this paper, we focus on concepts relating to the fifth and sixth steps, which have been studied in depth through the fields of atmospheric (McElroy, 2002; Seinfeld and Pandis, 1997) and environmental science (Bennett et al., 2002; Marshall et al., 2005). An important aspect of atmospheric physics for this paper is the concept of stability, which describes the degree of vertical mixing that occurs in the atmospheric boundary layer (ABL). A more unstable ABL allows for increased vertical dispersion and decreased concentration of pollutants. One of the primary contributors to the instability of the ABL is solar heating (Ahrens, 2003). Heating causes an increase in temperature and decrease in density of parcels of air at the Earth's surface. Consequently these parcels rise through surrounding air which is more dense, causing pollutants to be dispersed to higher altitudes. Pasquill stability classes have been the most widely used scheme for categorizing stability for several decades (Pasquill, 1961). Although

recently developed dispersion models have begun to use more detailed methods, the majority of models still use these classes and they provide a useful descriptive tool. An updated usage of Pasquill stability classes clearly indicates that daytime atmospheric instability increases with the level of solar radiation, and that the nighttime stability class is never less than that of daytime (Mohan and Siddiqui, 1998). Although the degree of influence of this phenomenon may vary, the ubiquitous effect of solar heating over the Earth's land masses makes it relevant for the majority of metropolitan areas.

This paper makes an investigation of this phenomenon and its influence on exhaust concentrations associated with nighttime metropolitan logistics policies. In Section 2, scenarios are presented for two locations in California, contrasting the extent to which estimated exhaust concentrations are affected depending on local meteorology. In Section 3, concepts of traffic flow theory are incorporated to assess environmental-policy implications of nighttime strategies under varying levels of congestion during the morning commute period. In addition, a discussion is provided, indicating the parallels between the impacts on diesel exhaust concentrations of nighttime policies those of other environmental concerns. Section 4 concludes the paper.

2. Influence of local meteorology on exhaust concentrations

$PM_{2.5}$ concentrations resulting from truck tailpipe emissions are quantified at two locations under hypothetical scenarios in which truck trips are shifted out of peak hours. The locations are in California in the vicinity of Interstate 880 (I-880) in Oakland and Interstate 580 (I-580) in Livermore. The meteorology of these two locations contrast, in that Oakland's is representative of coastal settings and Livermore's of inland settings. Inland weather patterns are not moderated by the ocean, which changes temperature more slowly than land, and as a result diurnal temperature variations are typically larger at inland locations. This phenomenon is made apparent by the probability distributions of hourly stability class for each location, as shown in Figure 1. The letters represent stability classes ranging from A, the most unstable, to F, the most stable.

Figure 1. Stability class probability distributions during the Summer
Source: (Bay Area Air Quality Management District, 2008)

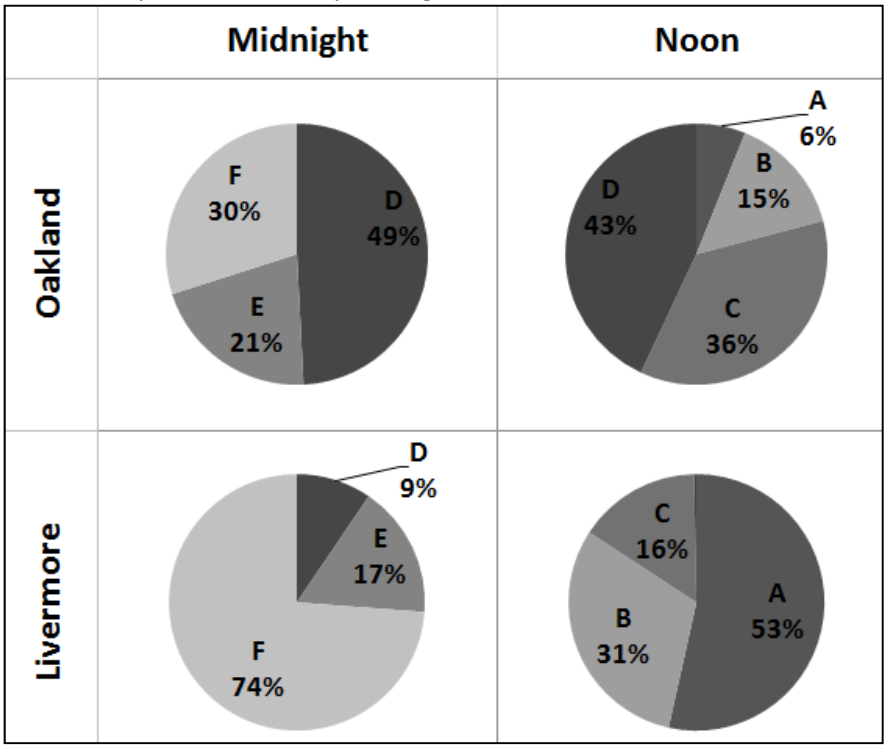

These locations are also representative of roadways that are heavily used by freight vehicles, since they service traffic associated with the Port of Oakland, which is currently the fourth busiest port in the United States (Port of Oakland, 2008). Recognizing the environmental impact associated with ports, the California Air Resources Board (CARB) has recently conducted a comprehensive study of diesel particulate impacts on the health of Oakland residents, based on current logistics operations (California Air Resources Board, 2008). Similar to CARB's study, the scenarios of section 2.2 provide estimates of particulate concentrations. The Port of Oakland has also conducted a trial program to explore the potential of night operations for mitigating congestion and air quality problems in the Bay Area and Central Valley (Port of Oakland, 2005).

2.1. Data and methodology

Multiple data sources and models are applied to estimate concentrations near I-880 and I-580. These data and models relate to traffic and dispersion modeling.

Traffic information is extracted from California Department of Transportation data (Caltrans, 2008), which provides both average annual daily aggregate and truck traffic. This daily information is converted to an hourly format by assuming a weekday hourly trip distribution. This distribution is derived from weigh-in-motion data for Monday through Thursday on San Francisco Bay Area highways and has been used in previous research (Dreher and Harley, 1998). Composite exhaust $PM_{2.5}$ emission factors, accounting for both trucks and other vehicles, are estimated using EMFAC2007 (California Air Resources Board, 2006) and the distribution of truck flows by axle class as specified in the Caltrans data. The formula for the estimation of composite $PM_{2.5}$ emission factors for a specific location and hour of the day is shown in Eq. 1. We note that the emission factors also vary by hourly average speeds, which are extracted from the PeMS database (PeMS, 2008). However, this has only minor effect in the two

scenarios considered in this paper, since hourly average speeds do not fall below 64 km/hr. Congestion effects are considered further in section 3.

$$EF_{CT} = \frac{Q_C \times e_C + \sum_{n=2}^{N} Q_{Tn} \times e_{Tn}}{Q_C + \sum_{n=2}^{N} Q_{Tn}} \quad \text{Eq. 1}$$

$EF_{CT} = composite\ emissions\ factor$

$e_{Tn} = logistics\ vehicle\ emissions\ factor\ for\ axle\ class\ n$

$e_C = passenger\ vehicle\ emissions\ factor$

$Q_{Tn} = hourly\ trips\ made\ by\ trucks\ of\ axle\ class\ n$

$Q_C = hourly\ trips\ made\ by\ other\ vehicles\ (primarily\ cars)$

$N = number\ of\ truck\ axles\ in\ highest\ axle\ class$

Values for the composite $PM_{2.5}$ emission factor and hourly vehicle trips are then applied in the Caltrans line source dispersion model, Caline4 (Benson, 1984; Benson, 1992), to estimate concentrations at various receptor locations. Additional inputs, such as aerodynamic surface roughness and hourly meteorology variables are extracted from meteorological data (Bay Area Air Quality Management District, 2008). The meteorological variables extracted are wind direction, wind speed, atmospheric stability class, standard deviation of wind direction and temperature. The mixing height is estimated according to the formula suggested by (Benson, 1984). All roadway geometry variables such as widths, lengths and locations of bridges are determined by use of Google Earth (Google, 2008a).

Concentrations of $PM_{2.5}$ are primarily dependent on atmospheric stability, wind direction and wind speed. In accordance with the literature, the expected concentration is calculated based on a joint distribution of these three variables (Pfafflin and Ziegler, 2006). This allows for the estimation of a

seasonal average based on a joint probability mass function (pmf) which is derived from the meteorological data. The pmf is created by categorizing wind speeds into 15 bins, each having an interval of 1 m/s and wind directions into 24 bins each having an interval of 15 degrees. Stability is categorized according to the six Pasquill classes. For each combination of these three variables, Caline4 is applied to estimate the concentration ($Conc^h$) for a given hour and receptor location. Subsequently, Eq. 2 is used to calculate the expected concentration ($E[Conc^h]$) for each hour and receptor location.

$$E[Conc^h] = \sum_{SC,WD,WS} Conc^h(sc, wd, ws, \bar{I}) \times p(sc, wd, ws) \quad \text{Eq. 2}$$

$Conc^h(sc, wd, ws, \bar{I})$

$= concentration\ at\ particular\ receptor\ location\ and\ hour\ h\ for\ stability\ class\ sc,$

$wind\ direction\ wd, wind\ speed\ ws, and\ a\ vector\ of\ constant\ inputs\ \bar{I}$

$p(sc, wd, ws) = probability\ mass\ function$

$SC = set\ of\ stability\ classes$

$WD = set\ of\ wind\ direction\ bins$

$WS = set\ of\ windspeed\ bins$

The contribution of the $PM_{2.5}$ concentration made by trucks is then calculated by multiplying $E[Conc^h]$ by the fraction of total emissions released by trucks (TC^h) during hour h. We note that Caline4 output $Conc^h$ values vary linearly with the input composite emission factor (Benson, 1984), so the value used for the car emission factor has no effect as long as TC^h is modified appropriately.

The 24-hour average $PM_{2.5}$ concentration ($E[Conc^{24}]$) is then calculated according to Eq. 3. $E[Conc^{24}]$ allows for comparison of the effects of shifting logistics operations to the night and is used by the EPA in

the designation of National Ambient Air Quality Standards (U.S. Environmental Protection Agency, 2008).

$$E[Conc^{24}] = \frac{1}{24} \times \sum_{h=1}^{24} TC^h \times E[Conc^h] \quad \text{Eq. 3}$$

$Conc^{24} = 24\text{-}hour\ average\ concentration$

$TC^h = fraction\ of\ emissions\ released\ by\ trucks\ during\ hour\ h$

Although $E[Conc^{24}]$ provides a basis for understanding the effects associated with off-peak operations, several additional factors influence health impacts. These include the diurnal variation in daily travel patterns, infiltration rates to indoor environments, and breathing rates. Eq. 4 is used to estimate 24-hour average pollutant intake ($E[Intake^{24}]$) for an individual remaining at a single receptor throughout the day.

$$E[Intake^{24}] = \frac{1}{24} \times \sum_{h=1}^{24} BR^h \times TC^h \times E[Conc^h] \quad \text{Eq. 4}$$

$Intake^{24} = 24\text{-}hour\ average\ intake$

$BR^h = breathing\ rate\ during\ hour\ h$

The methods of a previous study (Marshall, 2005; Marshall et al., 2003) that estimated pollutant intake in California are followed to define breathing rates and infiltration. Values for hourly breathing rates are taken directly from this study and exposure concentration is assumed to be equal to ambient concentration for nonreactive gases in most environments. All receptor locations used in section 2.2 qualify as being located in these types of environments, therefore outdoor and indoor concentrations of $PM_{2.5}$ released from trucks are assumed to be equal throughout the day.

In accordance with Eq. 4, the scenarios of section 2.2 will ignore the issue of daily travel patterns. However, we note that the receptor locations are in predominantly residential neighborhoods, in which there are likely to be more people during the night than the day. Therefore, estimates for $E[Intake^{24}]$ under hypothetical off-peak policies are likely to be biased downward.

2.2. Results

Figures 3 and 4 display estimates for $E[Conc^{24}]$ and $E[Intake^{24}]$ respectively, in Oakland for summer and winter at the receptor locations shown in Figure 2. Figures 5 through 7 present analogous information for Livermore. To allow for comparison, the results are produced for six different cases of daily truck trip distribution. These cases will be referred to alphabetically as case a through case f. Case a represents the status quo, whereas case b is based on a 24-hour uniform hourly distribution of truck trips. For cases c through f, the same total number of truck trips are shifted out of peak periods, but the times of the assumed peak and off-peak periods differ. Accordingly, a different percent of trips is removed from the peak hours for each case (and this percent is uniform across peak hours for each case). Moreover, trips are assumed to be uniformly added to the off-peak hours. The percent of trips shifted, and peak and off-peak times are displayed in the Figures 3-4 and 6-7.

For the remainder of section 2 we will refer to the percent changes in $E[Conc^{24}]$ and $E[Intake^{24}]$ for various cases versus case a, to draw comparisons relative to the status quo. Case c represents a situation in which truck trips are shifted out of daytime hours, similarly for examples to the congestion charging schemes in London (Transport for London, 2009) and Stockholm (Daunfeldt et al., 2009). Results for case c, as shown in Figures 3 and 6, indicate that nighttime logistics operations cause significantly larger relative increases in $E[Conc^{24}]$ at receptor locations in Livermore than in Oakland, in accordance with the variations in stability class shown in Figure 1. In addition, the changes during the summer are larger due to greater diurnal variation in prevailing meteorology. This results from

increased solar heating during summer, when there are more daylight hours and more intense sunlight during the day. The effect of wind direction is also notable, as the prevailing wind direction is from the southwest instead of northwest for a much higher fraction of the time during the night than the day in Oakland. Although concentrations at receptor 4 are generally low, the diurnal change in wind pattern results in a larger percent change in $E[Conc^{24}]$ at receptor 4 than the other receptors, since this intersection lies directly to the northwest of I-880. This fraction is also much greater during the winter than the summer. Case c, as shown in Figures 4 and 7, reveals that a shift of truck trips away from daytime hours does not generally improve $E[Intake^{24}]$ in Oakland, and is likley to worsen $E[Intake^{24}]$ in Livermore. These results are commensurate with the $E[Conc^{24}]$ increases shown in Figures 3 and 6.

Case d applies the peak and off-peak times currently utilized in the PierPASS system at the ports of Los Angeles and Long Beach (PierPASS, 2009). As can be seen in Figures 3 and 6, $E[Conc^{24}]$ for case d is generally less than that for case c, since case d shifts trips out of pre-dawn hours, when the ABL is very stable, and also the off-peak period begins slightly earlier, when the ABL is relatively unstable. However $E[Conc^{24}]$ for case d is greater than that for case a. Figures 4 and 7 show that $E[Intake^{24}]$ for cases a and d is comparable in Oakland, whereas $E[Intake^{24}]$ for case d is consistently higher than for case a in Livermore. These results indicate that the hours utilized in PierPASS are not likely to reduce diesel exhaust concentrations and may worsen human intake in many locations.

Cases e and f utilize alternative times for peak and off-peak periods to show what types of policies are more likely to ameliorate impacts. Case e removes trips from pre-dawn hours and the morning commute period, and shifts them to the current PierPASS off-peak period. This results in comparable or lesser values of $E[Conc^{24}]$ and $E[Intake^{24}]$. These results differ from case d, since trips are not shifted away from the late morning and afternoon, when the ABL is unstable. Case f is the same as case e, except that the off-peak period to which truck trips are shifted ends at 22:00, corresponding to the

decrease in port drayage activity after this time (BST Associates, 2008). The sharp drop in activity is associated with the 22:00-23:00 break taken by longshoreman. Although breathing rates are higher during the evening than the night, the results for case f generally indicate that there is a further reduction in $E[Conc^{24}]$ and $E[Intake^{24}]$ versus case e, since truck trips are shifted to earlier hours, when the ABL is less stable. Therefore, a focus on shifting off-peak operations to the evening instead of the night may allow both reduced health impacts and better utilization of labor.

Figure 2. I-880 and receptor locations 1-4 in Oakland
Source: (Google, 2008b)

Figure 3. Estimated $PM_{2.5}$ concentrations in Oakland

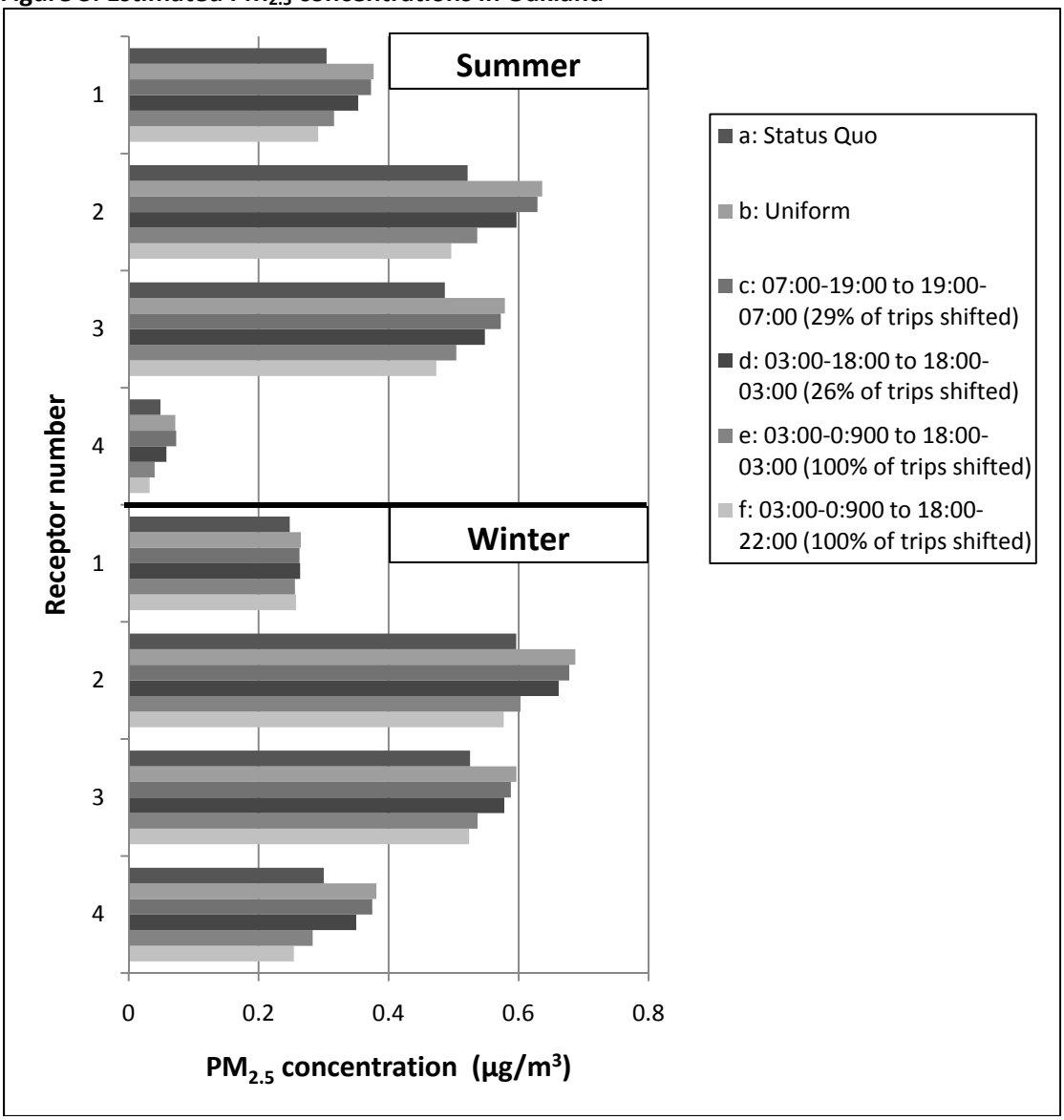

Figure 4. Estimated individual $PM_{2.5}$ intake in Oakland

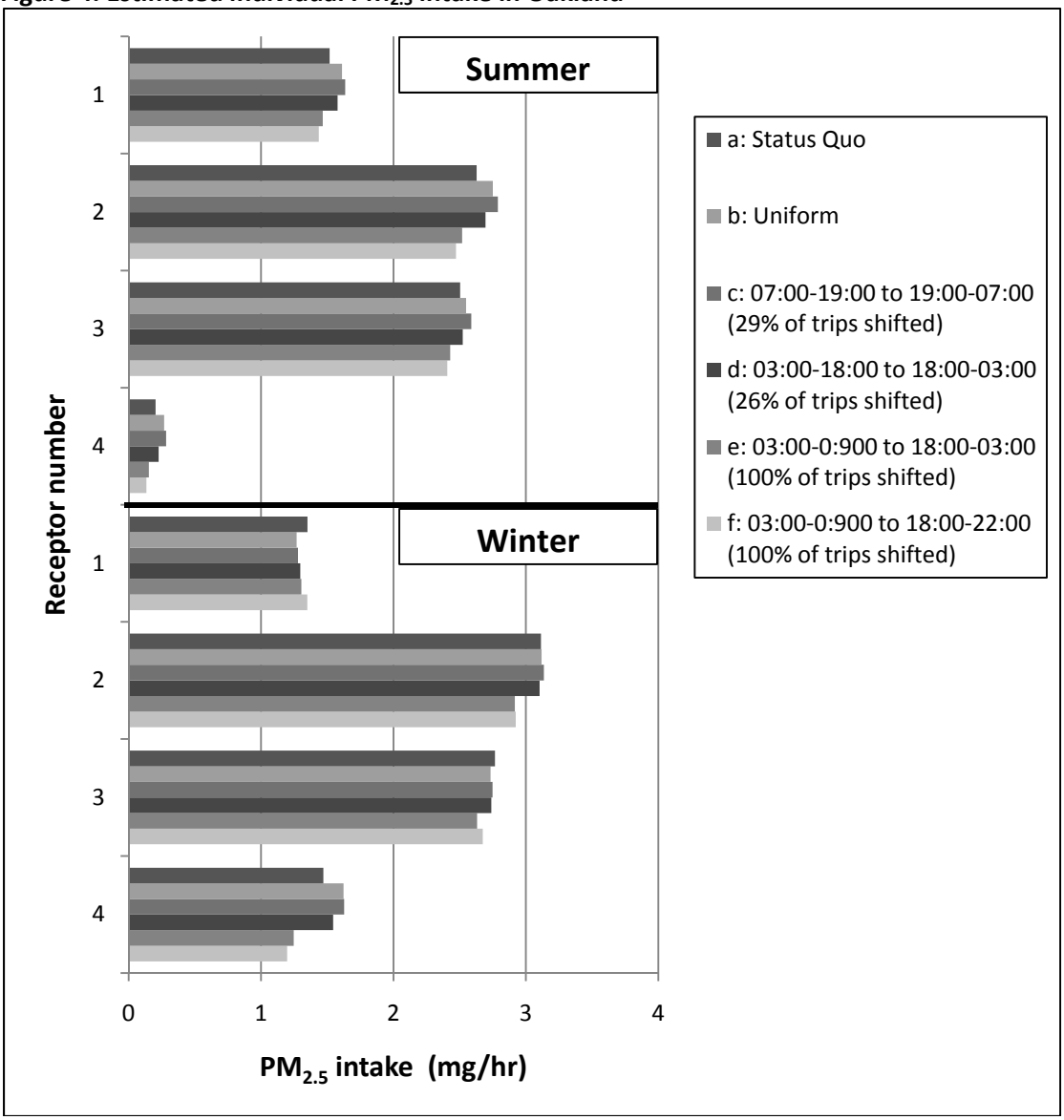

Figure 5. I-580 and receptor locations 1-3 in Livermore
Source: (Google, 2008b)

Figure 6. Estimated $PM_{2.5}$ concentrations in Livermore

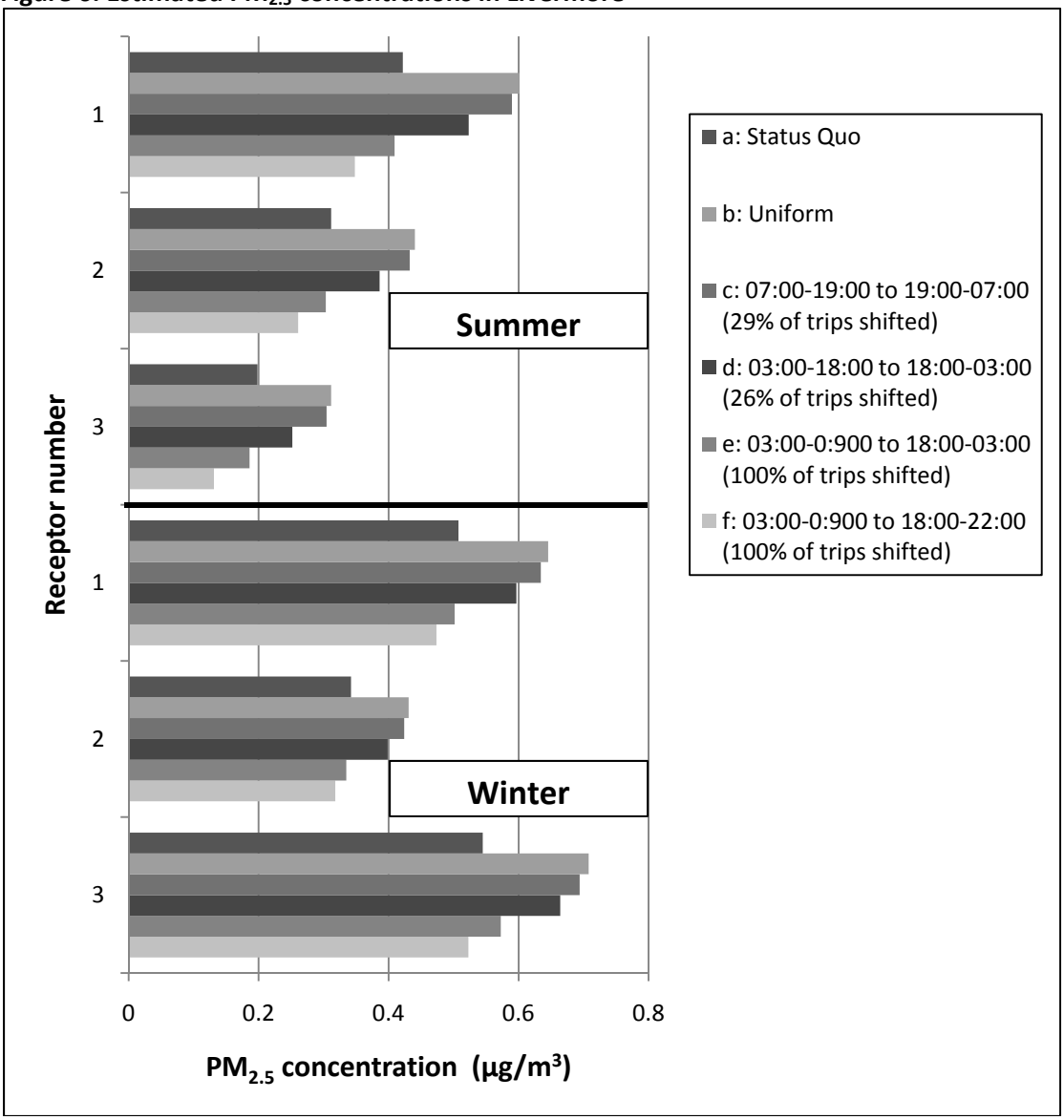

Figure 7. Estimated individual $PM_{2.5}$ intake in Livermore

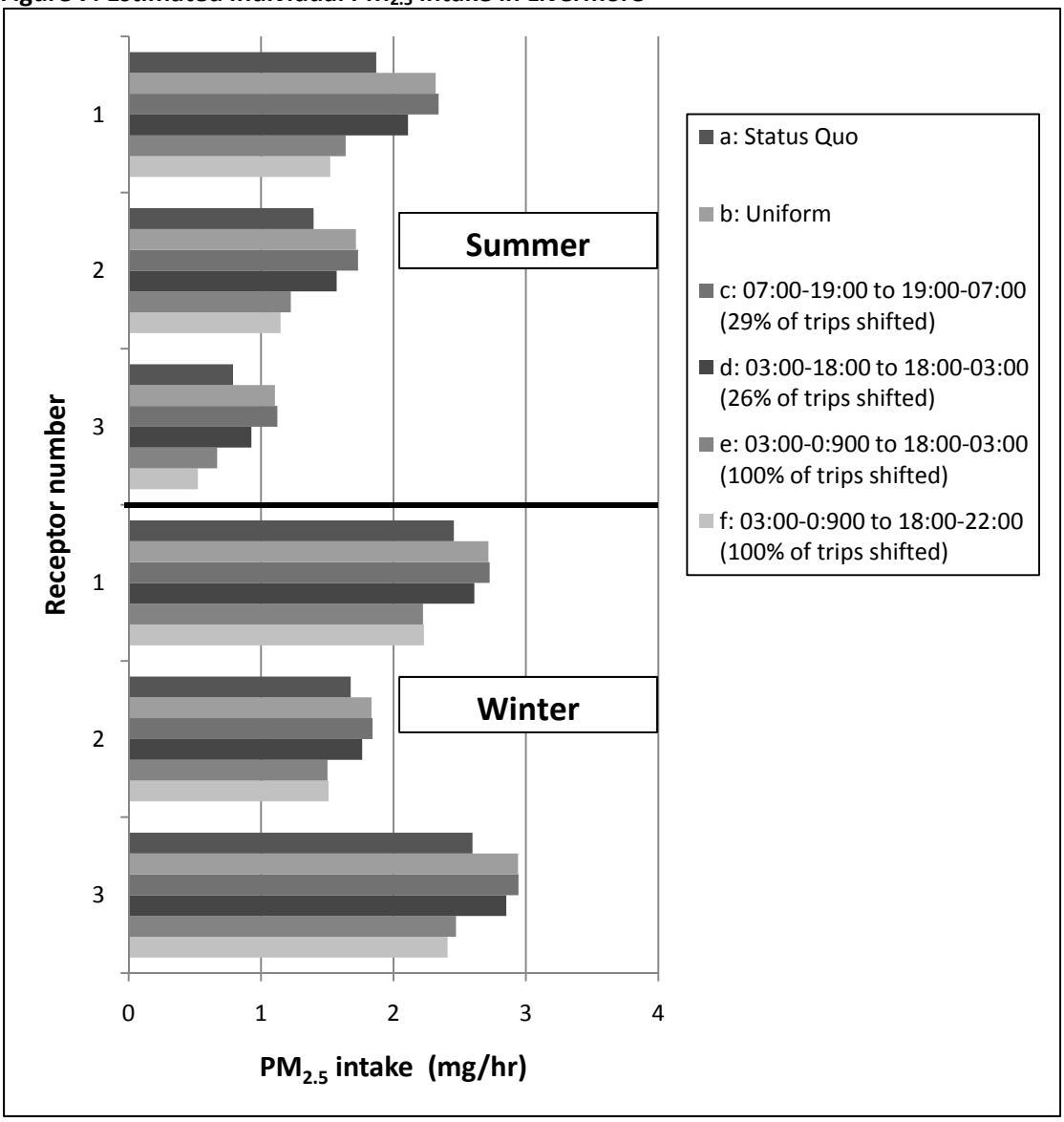

3. Accounting for traffic congestion

In section 2, we presented multiple scenarios, showing the effects of hourly variations in prevailing meteorology. However, as traffic speeds on the highway segments studied undergo little variation, only cursory investigation of congestion effects was made. As previously mentioned, congestion mitigation is a primary aim of policies for shifting freight trips to off-peak hours. Therefore, in section 3, we incorporate traffic considerations to provide further analysis of the types of situations in which unintended environmental impacts are likely to occur.

The analysis of section 2 is based on real-world scenarios, whereas in section 3 we utilize a more theoretical approach, in that hypothetical examples are used to develop insights. A graphical tool, in the form of a $PM_{2.5}$ concentration isopleth diagram, is used to analyze the various examples. Traffic flow theory is then used to enhance realism. We note that this paper does not account for congestion within terminals, for which other mitigation methods such as appointment systems are applicable (Giuliano and O'Brien, 2007).

3.1. Isopleth diagrams

A diagram containing isopleths of $PM_{2.5}$ concentration, averaged over a peak period and the night, is used to show how this value varies with respect to changes in the fraction of freight vehicle trips shifted to off-peak periods at a single bottleneck. The format of the diagram is shown in Figure 3. S^M can be understood to represent the speed of traffic during the peak period, although this definition will be further refined in section 3.3. FS represents the fraction of freight trips shifted to off-peak operations. Therefore, if we know S^M for a specific roadway link, one can see that a movement in the vertical direction from a point on the isopleth diagram would depict the change in average $PM_{2.5}$ concentration

resulting from increasing FS. The $PM_{2.5}$ concentration values could be replaced with human intake estimates or other environmental impacts.

Figure 8. Format of the isopleth diagram for off-peak policies

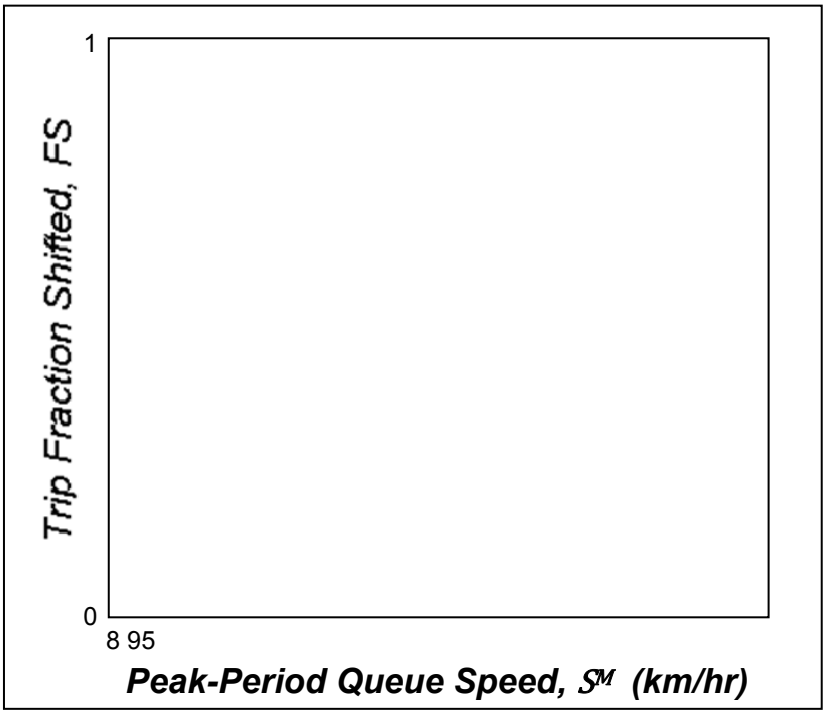

Several assumptions are made in this section, of which two will be pointed out here. The first is that the speed of traffic is constant during the peak period. This is justified by empirical evidence which shows that the level of congestion on roadways tends to be unaffected by a reduction in trip demand, although the time duration of the peak period may be reduced (Small, 1992). The second is that we are only dealing with a single bottleneck. Thus there may exist additional complexities for networks; however, logistics vehicles generally comprise an impacting fraction of traffic only at specific locations (Grenzeback et al., 1990). In addition, the analysis of a single bottleneck has often been used to develop intuition for more complicated scenarios (Daganzo, 1995a; Newell, 1987).

3.2. Emission factors and environmental considerations

The example of a one-direction, three-lane link with a wind direction of 270º, as depicted in Figure 4, is used to develop initial insights. A list of variables used in section 3.2 is shown in Table 1, since they are referred to multiple times in the text.

Table 1. Variables used in section 3.2

$Conc^h$	Caline4 output average $PM_{2.5}$ concentration for hour h
$Conc^Y$	Average $PM_{2.5}$ concentration during period Y
$D(t, FS)$	Departure curve
EF^Y	Composite $PM_{2.5}$ emission factor during period Y
e_X	$PM_{2.5}$ emission factor for vehicle type X
FS	Fraction of freight trips shifted to off-peak operations
k	Traffic density
k_c	Traffic critical density
k_j	Traffic jam density
N	Cumulative number of vehicles
O	Superscript used to denote original value of variable for FS^O (i.e. where $FS = 0$)
PCE	Passenger-car equivalent
Q_X^Y	Flow of vehicle type X during period Y
q	Traffic flow
q_c	Traffic capacity
S_{Trans}	Transition ${}_MS$ between improving and damaging traffic speed regimes
S^Y	Speed of queued traffic during period Y
s_f	Free-flow traffic speed
$T^Y(FS)$	Duration needed to serve traffic demand during period Y
T^{Yh}	Fraction of hour h used to serve trip demand during period Y
t	Time
TC^Y	Fraction of total traffic $PM_{2.5}$ emissions made by freight vehicles during period Y
TF^O	Fraction of peak-period trip demand comprised of freight vehicles for $FS = 0$ in units of passenger vehicles
TFV^O	Fraction of peak-period trip demand comprised of freight vehicles for $FS = 0$ in units of vehicles
$Time$	Averaging time for $PM_{2.5}$ concentration estimates
$V(t, FS)$	Virtual arrival curve for all vehicles
w	Traffic backward wave speed
X	$= \begin{cases} C\ if\ variable\ represents\ passenger\ vehicles \\ T\ if\ variable\ represents\ freight\ vehicles \\ CT\ if\ variable\ represents\ all\ vehicles \end{cases}$
Y	$= \begin{cases} M\ if\ variable\ represents\ peak\ period \\ N\ if\ variable\ represents\ night \\ MN\ if\ variable\ represnts\ average\ across\ peak\ period\ and\ night \end{cases}$
$Z_X^Y(FS)$	Trip demand during period Y for vehicle type X

The fundamental diagram (FD) displayed in Figure 10 is assumed to represent possible traffic states on the link. The FD is widely used to depict the relationship between traffic flow and density for a link

(Daganzo, 1997). In addition, the triangular FD is often used as an approximation and retains the necessary features for the purposes of this section. The approximation has also been shown to be reasonable empirically (Banks, 1989) and has been applied in seminal works on traffic flow theory (Newell, 1993). The FD in Figure 10 is defined by the following parameters:

$s_f = 97\frac{km}{hr}$, $k_j = 375\frac{car}{km}$, $q_c = 6000\frac{car}{hr}$, $k_c = 63\frac{car}{km}$, and $w = 19\frac{km}{hr}$.

The geometric interpretations of these parameters are indicated in Figure 10. The total trip demand ($Z_{CT}^{M}(FS)$) is assumed to be 6000 in units of cars. Freight vehicles are assumed to make up 20% of this demand in units of vehicles, and subsequently make up 43% in units of cars. The passenger car equivalent is assumed to be $PCE = 3$ to convert between passenger and freight vehicles.

Figure 9. Example link, receptor and wind direction

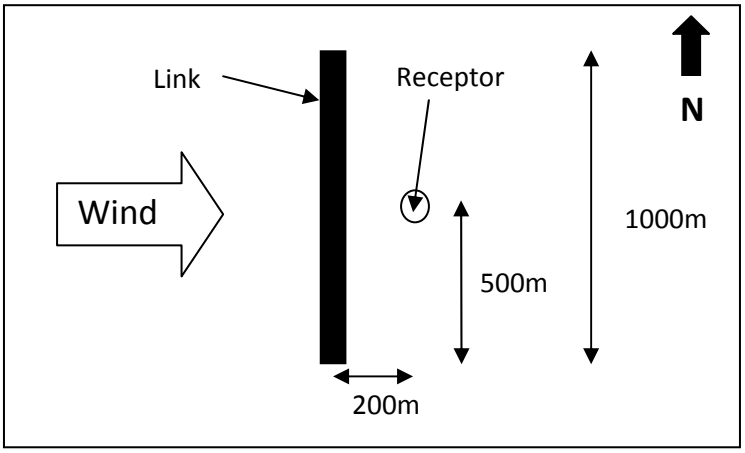

Figure 10. Example fundamental diagram

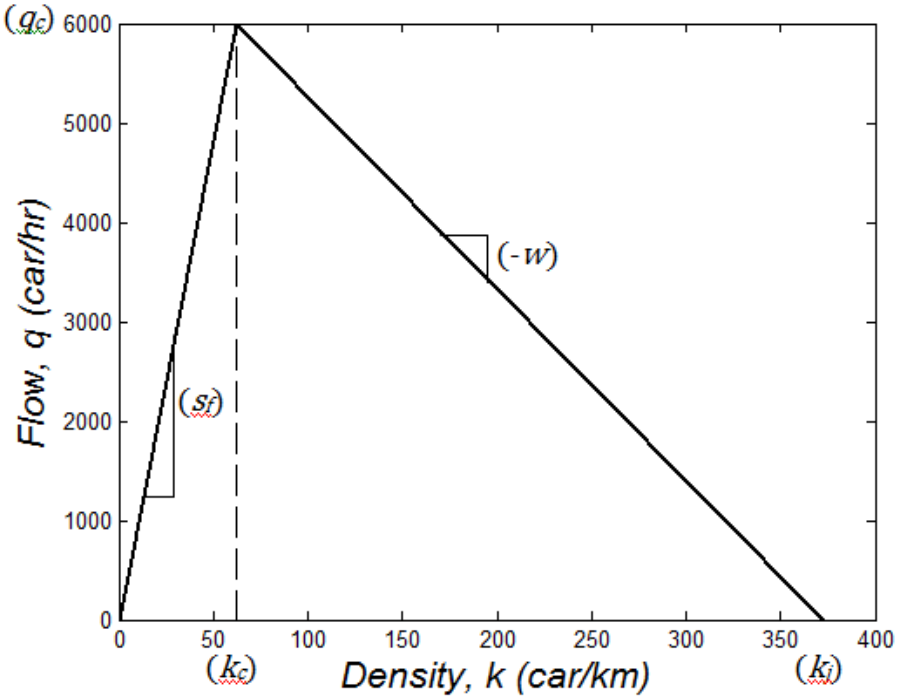

Vehicles are assumed to use the link shown in Figure 4 during the morning commute hour, starting at 08:00 and also during the night starting at 00:00. The demand at 08:00 corresponds to the morning commute problem with a single bottleneck, which has received much attention (Lago and Daganzo, 2007; Vickrey, 1969) as a basis for analyzing peak-period congestion. Freight trips are shifted from this

demand at 08:00 to travel at 00:00. Flow on the link is assumed to be constrained by a bottleneck at one end of the link and vehicles arrive at the back of the queue at the opposite end. Vehicles do not enter or exit the link at any other locations.

FS is increased from 0 to 1 to assess changes in the hourly concentration resulting from freight vehicles, averaged across the morning and night ($Conc^{MN}$). We assume this causes a change in the time ($T^M(FS)$) after 08:00 needed to serve morning trip demand ($Z_{CT}^M(FS)$), as shown in Figure 11, which is a cumulative plot for the bottleneck. The cumulative plot is commonly used in dynamic traffic analysis (Daganzo, 1997). $V(t, FS)$ represents the virtual arrival curve, and $D(t, FS)$ the departure curve, as a function of time, and also FS. For notational simplicity, the superscript O is used to indicate that $FS^O = 0$, which represents the original traffic situation prior to introduction of an off-peak policy. $Z_{CT}^M(FS)$ includes both passenger and freight trips. Note the sets of curves for FS^O and FS when $FS > FS^O$ coincide along much of the plot.

Figure 11. Cumulative plot for bottleneck with instantaneous link loading

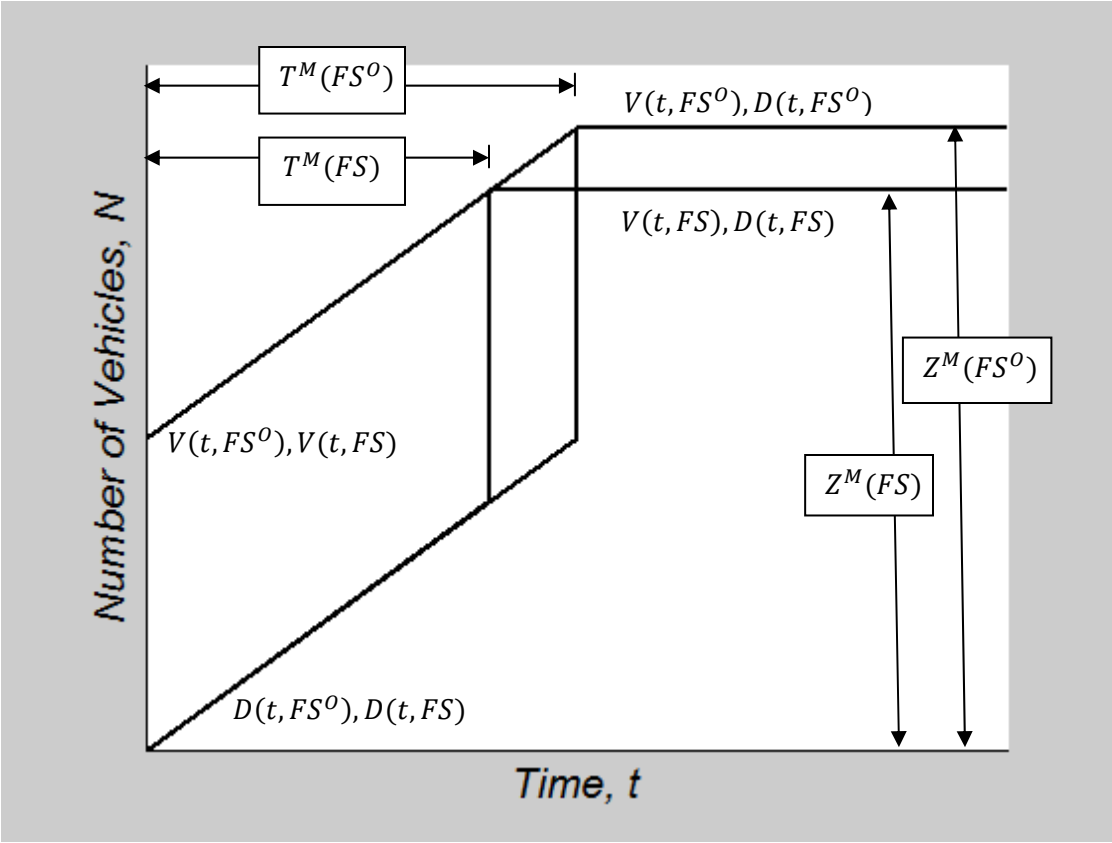

In accordance with Figure 11, the spatial extent of the queue, represented by the vertical distance between $V(t, FS)$ and $D(t, FS)$, is assumed to remain constant and equal to the length of the link throughout the duration of the morning analysis period. This is akin to assuming that the link is instantaneously filled and emptied of vehicles and that the arrival rate to the back of the queue is constant and equal to the departure rate at the bottleneck during the peak period. Another interpretation of this assumption is that the time during which the queue forms and dissipates is not accounted for and that the arrival rate is constant between these periods. Despite the lack of realism, this assumption is generally inherent in line source dispersion models, such as Caline4 (California Air Resources Board, 2006), in which steady-state traffic is assumed. Accounting for the varying spatial extent of the queue would greatly complicate dispersion modeling, since concentrations would have to be estimated at much finer time steps. The nighttime traffic speed (S^N) is assumed to be equal to s_f

and the time to service night truck demand ($T^N(FS)$) is used analogously to the use of $T^M(FS)$. The assumptions inherent in this setup simplify the development of the examples in this section without hindering their purpose. In addition, the examples can also be interpreted as worst case situations, since shifted traffic is assumed to have no effect on emissions or speeds for the remaining vehicles during the morning.

Figure 12, and Figure 14 through Figure 16 present isopleth diagrams for $Conc^{MN}$ in units of $\mu g/m^3$, as a function of S^M and FS. Mean summer climate characteristics are assumed, with the exceptions of wind direction, which is assumed as 270º, and stability class, for which the median is used. For illustrative purposes, the concentration intervals between the isopleths in these diagrams are not constant. However they are evenly spaced within a lower and a higher range of $Conc^{MN}$ values. The arrows on the diagrams point in the direction of decreasing $Conc^{MN}$.

The derivation of the formulas used to calculate $PM_{2.5}$ concentration values for the isopleths of Figure 12 and Figure 14 through Figure 16 can be seen in Eq. 5 through Eq. 16. Eq. 5 is used to compute w based on q_c , k_j , k_c , which are assumed from the FD in Figure 10.

$$w = \frac{q_c}{k_j - k_c} \qquad \text{Eq. 5}$$

w is then used along with k_c and q_c in Eq. 6 to calculate the morning flow (Q_{CT}^M). S^M takes on a range of assumed values, in accordance with the horizontal axis of the associated isopleth diagram. Therefore Eq. 6 is applied for multiple values of S^M to compute the associated Q_{CT}^M values.

$$Q_{CT}^{M} = \frac{q_c + w \times k_c}{1 + w/S^M} \quad \text{Eq. 6}$$

The fraction of all morning commute trips initially made up by freight vehicles (TFV^O) in units of vehicles is then converted to its equivalent in units of cars (TF^O) by applying $PCE = 3$, as shown in Eq. 7.

$$TF^O = \frac{TFV^O \times PCE}{TFV^O \times PCE + 1 - TFV^O} \quad \text{Eq. 7}$$

TFV^O is subsequently used to compute morning flows of freight vehicle traffic (Q_T^M) and car traffic (Q_C^M), as shown in Eq. 8 and Eq. 9. The second case of each equation is used when $FS \times TF^O < 1$, representing a situation in which less than 100% of freight trips have been shifted. To maintain the generality of the equations, the first case formulas are shown for $FS \times TF^O = 1$, since otherwise the denominator could equal 0.

$$Q_T^M = \begin{cases} 0 & if\ FS \times TF^O = 1 \\ \dfrac{(1 - FS) \times TF^O}{1 - FS \times TF^O} \times Q_{CT}^M & otherwise \end{cases} \quad \text{Eq. 8}$$

$$Q_C^M = \begin{cases} Q_{CT}^M & if\ FS \times TF^O = 1 \\ \dfrac{(1 - TF^O)}{1 - FS \times TF^O} \times Q_{CT}^M & otherwise \end{cases} \quad \text{Eq. 9}$$

The flow of nighttime traffic (Q_{CT}^N), is assumed to be equal to q_c and the flow of freight vehicle traffic (Q_T^N), since nighttime trip demand by cars is assumed to be 0. This is shown in Eq. 10.

$$Q_T^N = Q_{CT}^N = q_c \quad \text{Eq. 10}$$

The composite emission factors ($EF^Y, where\ Y = M\ or\ N$) for input to Caline4 are then computed as shown in Eq. 11. Note that Y is used to save on notation, and indicates that the variable is computed for both morning and night.

$$EF^Y = \frac{\frac{e_T}{PCE} \times Q_T^Y + e_C \times Q_C^Y}{Q_T^Y + Q_C^Y} \quad \text{Eq. 11}$$

$where\ Y = \begin{cases} M\ if\ morning \\ N\ if\ night \end{cases}$

EF^Y and the corresponding total vehicle flows (Q^Y) are then input into Caline4. TC^Y is then calculated through the use of Eq. 12, to distinguish the $PM_{2.5}$ concentration resulting from freight vehicles, versus that from cars. TC^Y is later used in Eq. 16.

$$TC^Y = \frac{\frac{e_T}{PCE} \times Q_T^Y}{\frac{e_T}{PCE} \times Q_T^Y + e_C \times Q_C^Y} \quad \text{Eq. 12}$$

$T^M(FS)$ and $T^N(FS)$ are calculated as shown in Eq. 13 and Eq. 14.

$$T^M(FS) = \frac{Z_{CT}^M \times (1 - FS \times TF^O)}{Q^M} \quad \text{Eq. 13}$$

$$T^N(FS) = \frac{Z_{CT}^M \times (FS \times TF^O)}{Q^N} \quad \text{Eq. 14}$$

Caline4 concentration outputs ($Conc^h$), which vary with inputs Q^Y and EF^Y, are applied in Eq. 16 to estimate the average concentration, $Conc^{MN}$, over an assumed averaging period of time ($Time$). We assume $Time = 6\ hours$, since $T^M(FS)$ exceeds 4 hours for the slowest travel speed for which Caline4 is applied, 8 km/hr, and $T^N(FS)$ is always less than 1 hour. $T^{Yh}(FS)$ represents the fraction of an hour, denoted by h, that is used to service trip demand. $T^{Yh}(FS)$ is calculated using Eq. 15. $T^{Yh}(FS)$ is equal to 1 for every hour except for the last hour of the morning commute and night traffic periods. We note that in the case that the duration of either of these periods is less than 1 hour, the associated value of $T^{Yh}(FS)$ would by default be less than 1 hour. Therefore the first case of Eq. 15 is applied when

considering the last hour of the morning or night periods, or if they last less than 1 hour. $T^{Yh}(FS)$ can subsequently then be used to assign less weight to these hours as shown in Eq. 16. The second case of Eq. 15 is used for all other periods.

$$T^{Yh}(FS) = \begin{cases} T^{Y}(FS) - \lfloor T^{Y}(FS) \rfloor & if\ \lfloor T^{Y}(FS) \rfloor = h - s \\ 1 & otherwise \end{cases} \quad \text{Eq. 15}$$

$$where\ s = \begin{cases} 0\ if\ Y = N \\ 8\ if\ Y = M \end{cases}$$

$$h = hour\ of\ the\ day\ assumed\ to\ be\ represented\ by\ an\ integer\ (e.g. 08{:}00\ to\ 09{:}00 \equiv 8)$$

Eq. 16 is used to calculate $Conc^{MN}$. The inner summation adds the hourly $PM_{2.5}$ concentrations resulting from freight vehicles within either the morning or the night period. The outer summation is then used to add across both the morning and night. The sum is then divided by $Time$ to derive an average concentration, $Conc^{MN}$.

$$Conc^{MN} = \frac{\sum_{Y=\{M,N\}} \sum_{h=s}^{s+\lceil T^{Y}(FS) \rceil} Conc^{h}(Q^{Y}, EF^{Y}, \bar{I}) \times T^{Yh}(FS) \times TC^{Y}}{Time} \quad \text{Eq. 16}$$

Several factors influence the form of the isopleth diagrams. These factors lead to regimes, characterized by the two arrows in Figure 12 and Figure 14 through Figure 16. In the lower S^{M} regime (Regime I) off-peak policies improve $Conc^{MN}$, whereas in the higher S^{M} regime (Regime D), $Conc^{MN}$ increases and environmental damage occurs. Regime D corresponds to the examples of section 2.2. S_{Trans} is used to refer to the transition value of S^{M} at which $\frac{\partial Conc^{MN}}{\partial S^{M}} = 0$, as shown in Figure 12.

Relatively high morning emission factors (EF^{M}) outweigh the effects of a stagnant nighttime ABL in Regime I (i.e. $\partial(Conc^{N} \times T^{N})/\partial FS < -\partial(Conc^{M} \times T^{M})/\partial FS$). However, EF^{M} decreases with S^{M} in

Regime I as shown in Figure 13. (i.e. $\partial EF^M/\partial S^M \leq 0$). This decrease results in the presence of Regime D where $S^M > S_{Trans}$ and $Conc^{MN}$ increases with FS (i.e. $\partial(Conc^N \times T^N)/\partial FS > -\partial(Conc^M \times T^M)/\partial FS$). Note that $Conc^{MN}$ also increases with S^M, for S^M greater than about 72 km/hr, since e_T increases in this regime, in accordance with Figure 13 (i.e. $\partial e_T/\partial S^M > 0 \Rightarrow \partial Conc^{MN}/\partial S^M > 0$). This results in the upside down u-shape of the isopleths at S^M = 72 km/hr.

Figure 12. $PM_{2.5}$ Isopleths (µg/m^3) for summer in Oakland with free-flow speed, $s_f = 97\ km/hr$

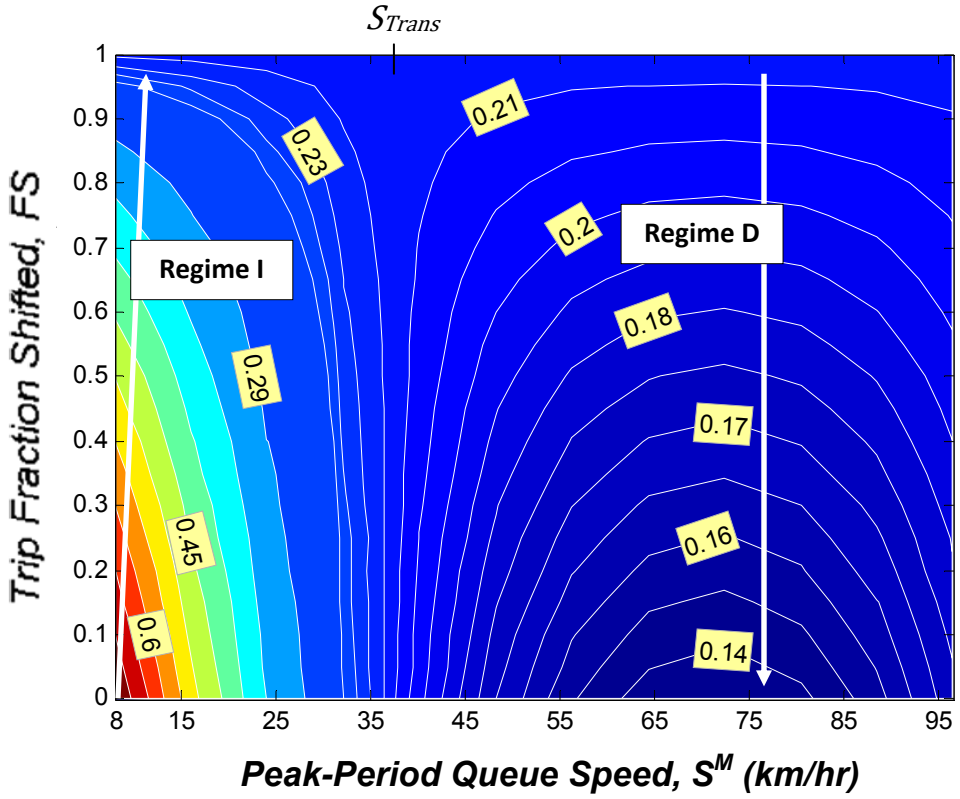

Figure 13. EMFAC2007 Heavy-heavy duty vehicle $PM_{2.5}$ emission factors for Alameda County

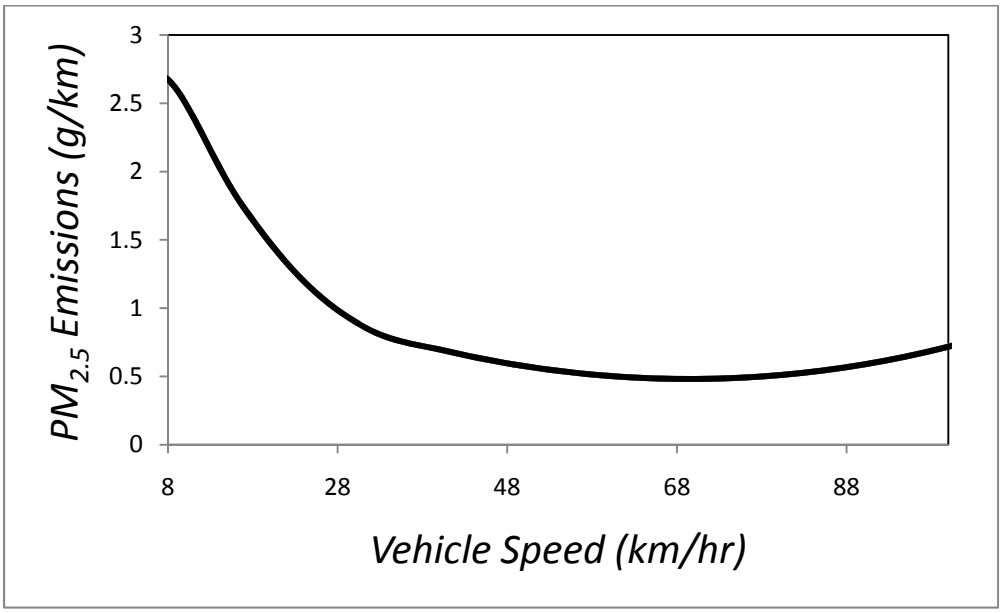

Figure 14 presents the resulting isopleth diagram for the same situation used to produce Figure 12, except that s_f is reduced to 64 km/hr. This lower s_f represents the case of arterials or collectors, instead of highways. The FD is accordingly adapted so that q_c is reduced, and k_c increased. As can be seen, S_{Trans} is higher, because the reduction in s_f causes a decrease in EF^N, as shown in Figure 13. This suggests that nighttime policies are more likely to be beneficial for cases in which S^N is lower. However, Figure 15 shows the case in which s_f is reduced to 32 km/hr, which indicates that S_{Trans} is lower. This is in accordance with the increasing EF^N associated with decreasing S^N lower than about 72 km/hr as shown in Figure 13. Nevertheless, S_{Trans} is fairly close to s_f, so reduced $Conc^{MN}$ could still likely be achieved for links with very low s_f.

Figure 14. $PM_{2.5}$ Isopleths (µg/m^3) for summer in Oakland with free-flow speed $s_f = 64\ km/hr$

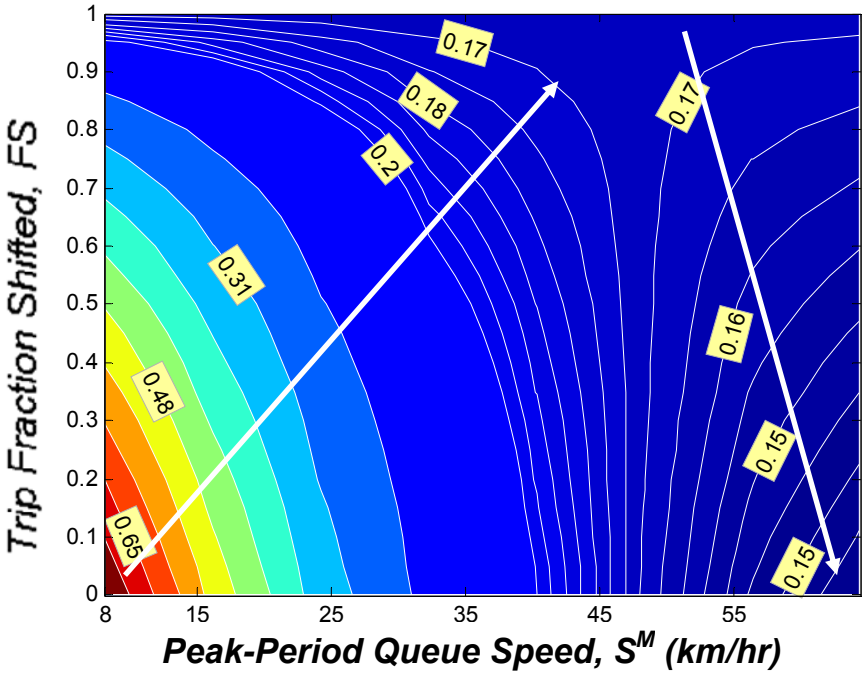

Figure 15. $PM_{2.5}$ Isopleths (µg/m^3) for summer in Oakland with free-flow speed, $s_f = 32\ km/hr$

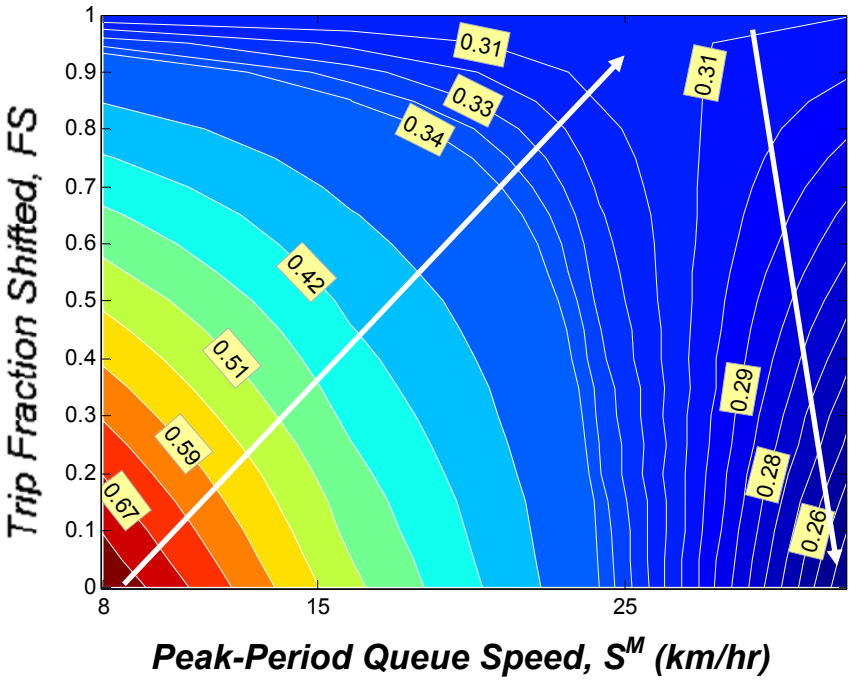

Figure 16 is again produced using the situation depicted in Figure 4 through Figure 11. However, typical climatic conditions for the summer in Livermore are used. Consequently, the value for S_{Trans} is lower than for Oakland, since the diurnal climate variation is more extreme. Consistent with the higher changes in $E[Conc^{24}]$ values found for Livermore in section 2, these results indicate that unintended environmental impacts are more likely to occur in inland climates in California.

Figure 16. $PM_{2.5}$ Isopleths (µg/m^3) for summer in Livermore with free-flow speed, $s_f = 97km/hr$

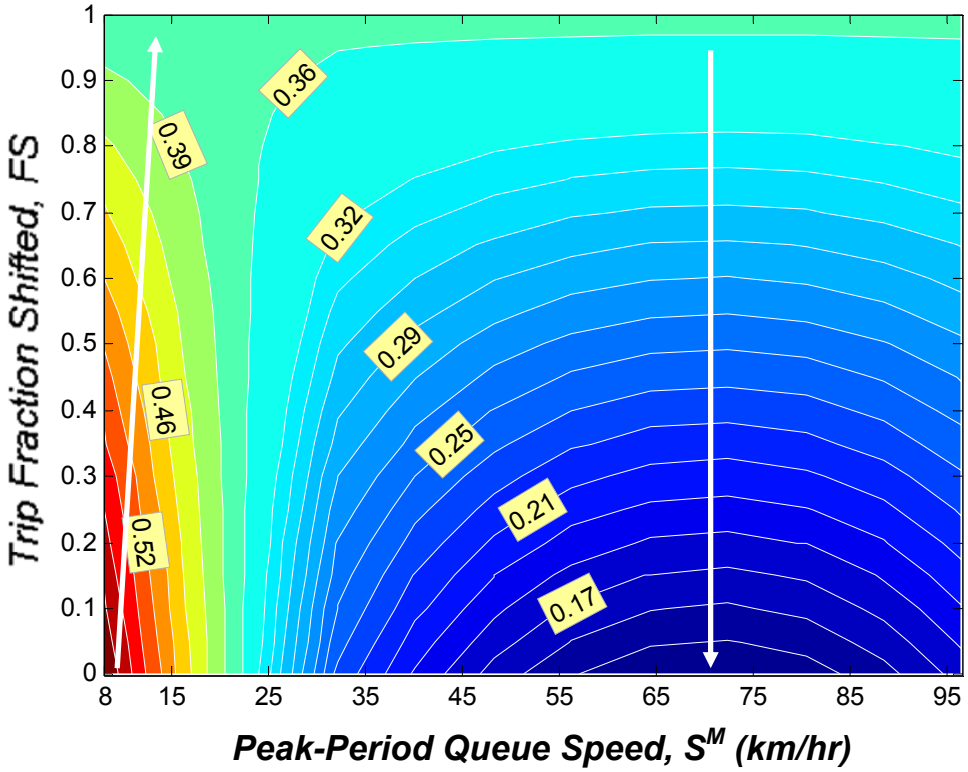

3.3. Decreasing marginal emissions benefits

This section expands upon the ideas presented in the isopleth diagrams of section 3.2. In addition to the atmospheric stability and emission factors, traffic effects are also incorporated. Traffic flow theory is used to exhibit the existence of decreasing marginal congestion benefits for freight vehicle emissions as a result of off-peak operations at a single bottleneck. This occurs since there is a decrease in the marginal time spent in queue by freight vehicles W_T, during which speeds are relatively low and

emission factors are high. Therefore, under the reasonable assumption that $Conc^N$ increases linearly with FS, there exist decreasing marginal environmental benefits as well (i.e. $\frac{\partial^2 Conc^{MN}}{\partial FS^2} > 0$). The assumption of linearly changing $Conc^N$ is refined in section 3.4, although it does not hinder the development of intuition at this point. Figure 12 provides graphical intuition of this tradeoff, for which $Conc^{MN}$ is minimized by FS^* at which $\frac{\partial(Conc^M \times T^M)}{\partial FS} = -\frac{\partial(Conc^N \times T^N)}{\partial FS}$. On the other hand, a linearly changing $Conc^M$ would result in either $FS^* = 0 \; if \; \frac{\partial(Conc^M \times T^M)}{\partial FS} > -\frac{\partial(Conc^N \times T^N)}{\partial FS}$ or $FS^* = 1 \; if \; \frac{\partial(Conc^M \times T^M)}{\partial FS} < -\frac{\partial(Conc^N \times T^N)}{\partial FS}$, as in the isopleth diagrams of section 3.2. A list of variables introduced in section 3.3 is shown in Table 2.

Table 2. Variables introduced in section 3.3

$D^E(t, FS)$	Extrapolated departure curve
FS^*	The value of FS^* which gives minimum ${}_{MN}Conc$ for a given ${}_{M}S$
FS_{Trans}	Transition FS between improving and damaging regimes
O	Superscript used to denote original value of variable (i.e. for which $FS = 0$) for t_0^O and t_1^O
t_0	Time at which first vehicle is delayed
t_1	Time at which last vehicle is delayed
t_{min}	Time when queue has minimum length between peak periods
τ	Total delay time incurred by all vehicles
μ	Departure rate (= $\frac{\partial D(t,FS)}{\partial t}$)
W	Total time spent in queue incurred by all vehicles
W_T	Total time spent in queue incurred by freight vehicles
Z_X	Trip demand of vehicle X

Figure 17. Graphical intuition of tradeoff between day and night concentrations

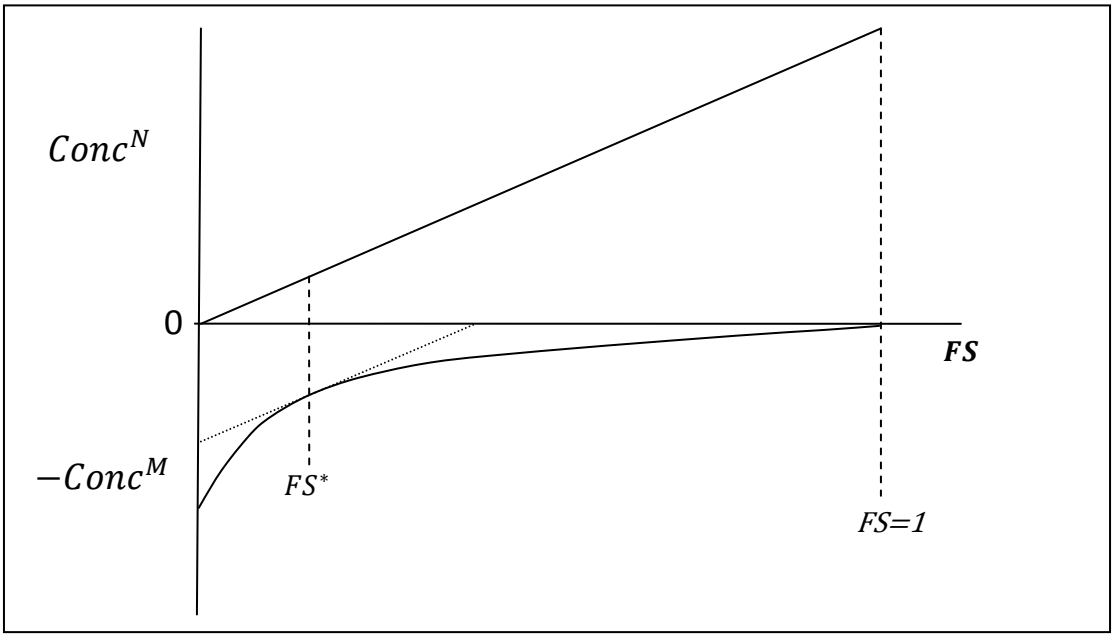

The decreasing marginal benefits will be shown to occur for the case of a single bottleneck with proportional trip demand reduction across time. As a result, there exists a value of FS_{Trans} for a given S^M, at which off-peak operations can switch from improving to damaging the environment. Subsequently there is likely to exist an additional regime which can be intuited from traffic flow theory (Regime T), in which increasing FS can damage the environment after prior increases lead to improvements. The corresponding isopleth diagram has three regimes and a FS_{Trans} line as exhibited in Figure 13. We note that decreasing marginal benefits have often been inherently assumed in the form of increasing, convex link performance functions (Sheffi, 1985; Zhang and Ge, 2004). However this assumption has been shown to be generally questionable, especially for heavily congested conditions (Daganzo, 1995b; Verhoef, 2005), which are of primary interest. Pertaining to this paper, a convex link performance function would imply a reduction in traffic flow as FS is increased, which would contradict these studies. Therefore we make use of a cumulative plot for a single bottleneck to describe the decreasing marginal benefits.

Figure 18. Hypothetical isopleths which account for decreasing marginal benefits to traffic congestion

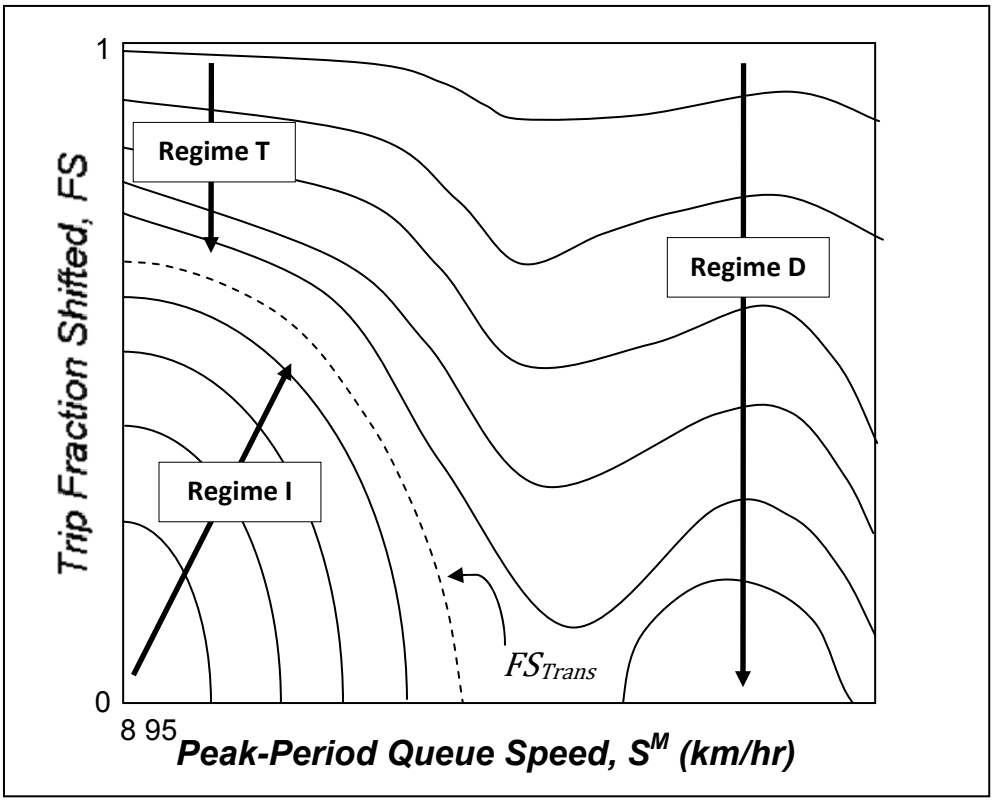

Next, a mathematical description of the problem of showing the existence of decreasing marginal benefits for a single bottleneck is presented. The S-shaped virtual arrival curves in Figure 19 are commonly used to represent a bottleneck during a single peak period (Daganzo, 1997). As can be seen $V(t, FS)$ has an earlier time period during which $\frac{d^2V(t,FS)}{dt^2} > 0$ until a point of inflection after which time $\frac{d^2V(t,FS)}{dt^2} < 0$. There is assumed to be some time interval, containing the point of inflection during which $\frac{\partial V(t,FS)}{\partial t} > \frac{\partial D(t,FS)}{\partial t}$. In addition it is assumed that $V(t, FS) \geq 0 \; \forall \; t$, $\frac{dV(t,FS)}{dt} \geq 0 \; \forall \; t$ and that $V(t, FS)$ is differentiable $\forall \; t$. The last assumption is in accordance with the commonly used fluid model for traffic (Daganzo, 1997). The departure rate, $\mu = \frac{dD(t,FS)}{dt}$, is assumed to be positive (i.e $\mu > 0$) and constant (i.e $\frac{d\mu}{dt} = 0$). The departure curve $D(t, FS)$ intersects $V(t, FS)$ at a point t_0 such that $\frac{dD(t_0,FS)}{dt} = \frac{dV(t_0,FS)}{dt}$, which is the time when the first vehicle is delayed. In addition they intersect later at t_1 when the last

delay occurs. Accordingly, $t_0 < t_1$ is assumed, since otherwise the problem would not correspond to anything practical. The increase of FS is assumed to cause a proportional decrease in $V(t, FS)$, (i.e. $(1 - TFV^O \times FS) \times V(t, FS^O) = V(t, FS)\ \forall\ t$). Of note is that the change in emissions with respect to FS for vehicles represented in Figure 19 differ from those in Figure 11, since the spatial extent of the queue varies with FS. This can be inferred from Figure 19, since $d(V(t, FS) - D(t, FS))/dt \neq 0$. This corresponds to the fact that, under congested conditions, a trip shifted to the off-peak period affects not only the emissions of that particular vehicle, but also the emissions of the remaining traffic during the peak period.

Figure 19. Virtual arrival and departure curves for five values of FS

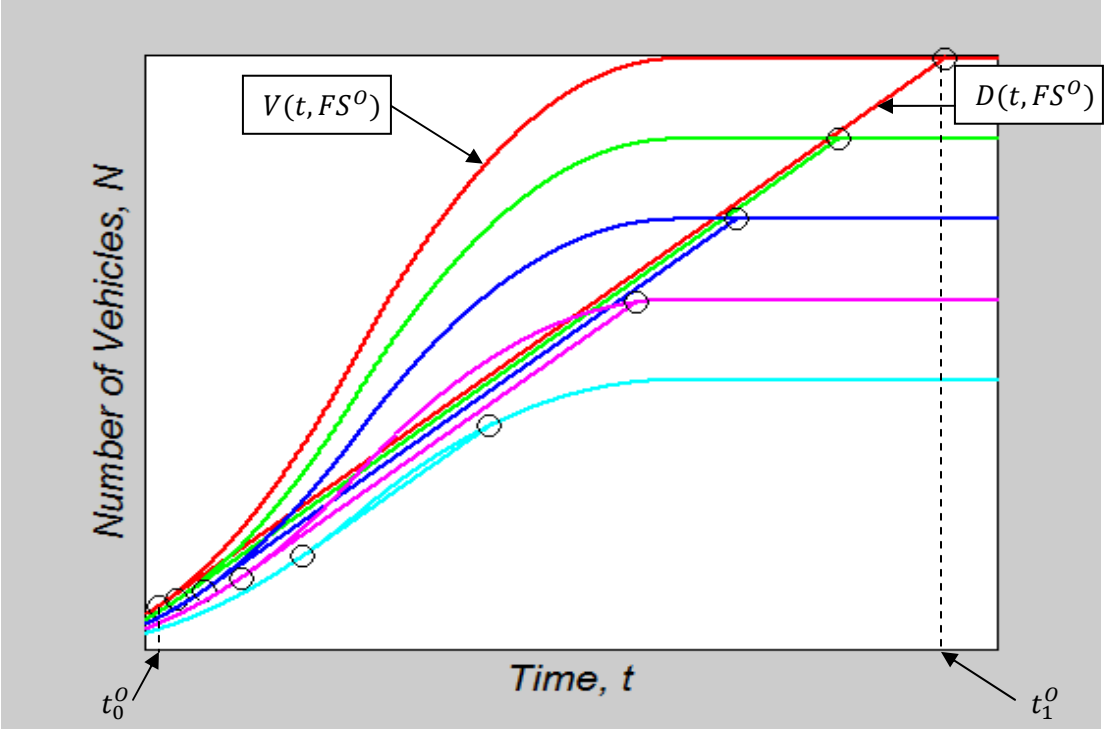

Next an equation for the total time spent in queue by logistics vehicles is presented. The area between $V(t, FS)$ and $D(t, FS)$, with endpoints at t_0 and t_1 represents the total delay to all vehicles τ, which is equal to the third term in parentheses of Eq. 17. In order to save on notation, the superscript O is used

to indicate that t_0^O and t_1^O are the endpoints of the queuing period for the original traffic situation (i.e. in which $FS = 0$). τ is linearly related to the total time spent in queue by all vehicles (W), which gives the first term in parentheses of Eq. 17 (Daganzo, 1997). The second term of Eq. 17 is the fraction of freight vehicles on the roadway, which is assumed to be constant across time. $Z_T(FS^O)$ and $Z_C(FS^O)$ are the initial values (i.e. for $FS = 0$) for the peak period trip demand of freight vehicles and cars, respectively. The product of the three terms in parentheses is equal to the total time spent in queue by freight vehicles W_T. Emission factors are generally higher in queued than free-flow traffic, according to Figure 13. Therefore one can also assume that $\frac{\partial^2 W_T}{\partial FS^2} > 0 \Rightarrow \frac{\partial^2 Conc^{MN}}{\partial FS^2} > 0$.

$$W_T = \left(1 - \frac{S^M}{s_f}\right)\left(\frac{Z_T(FS^O) \times (1 - FS)}{Z_T(FS^O) \times (1 - FS) + Z_C(FS^O)}\right)\left(\int_{t_0}^{t_1} [V(t, FS) - D(t, FS)]dt\right) \qquad \text{Eq. 17}$$

In addition, we know that $\frac{\partial^2 \tau}{\partial FS^2} > 0 \Leftrightarrow \frac{\partial^2 W}{\partial FS^2} > 0$, which is justified by the linear relationship between τ and W. Furthermore $\frac{\partial^2 W}{\partial FS^2} > 0 \Rightarrow \frac{\partial^2 W_T}{\partial FS^2} > 0$, since decreasing benefits to all vehicles implies decreasing benefits for the remaining freight vehicles, which comprise a declining fraction of traffic flow as FS is increased. Therefore we know that $\frac{\partial^2 \tau}{\partial FS^2} > 0 \Rightarrow \frac{\partial^2 W}{\partial FS^2} > 0 \Rightarrow \frac{\partial^2 W_T}{\partial FS^2} > 0 \Rightarrow \frac{\partial^2 Conc^{MN}}{\partial FS^2} > 0$. Thus if we know that $\frac{\partial^2 \tau}{\partial FS^2} > 0$, then there can exist decreasing marginal benefits for average $PM_{2.5}$ concentrations resulting from freight vehicle emissions, caused by increased off-peak trips. The proof of $\frac{\partial^2 \tau}{\partial FS^2} > 0$ can be intuited from the graphical construction shown in Figure 19. Nevertheless it is shown below, since the formulas therein are also used in subsequent discussion. In addition, following the justification for previous analytical studies of a single bottleneck (Newell, 1987), a step towards a theory may help identify what information is likely to be relevant and what policy inferences can be made in the future.

This is especially true for the environmental policy-making arena, which has not previously given significant attention to the subtleties of traffic effects.

Proof that $\frac{\partial^2 \tau}{\partial FS^2} > 0$:

Eq. 18 presents the typical delay formula for a bottleneck, although it is adapted to be a function of FS. Note that the limits of the integral are also dependent on FS, however this is not explicitly denoted to avoid confusion in later stages of the proof.

$$\tau = \int_{t_0}^{t_1} [V(t, FS) - D(t, FS)]dt \qquad \text{Eq. 18}$$

Next the first derivative is shown in Eq. 19, as a result of Leibniz integral rule:

$$\underbrace{\frac{d\tau}{dFS}}_{\leq 0} = \underbrace{\int_{t_0}^{t_1} \frac{\partial V(t, FS)}{\partial FS} - \frac{\partial D(t, FS)}{\partial FS} dt}_{<0} + \left[\underbrace{V(t_1, FS) - D(t_1, FS)}_{=0}\right] \frac{dt_1}{dFS} \qquad \text{Eq. 19}$$
$$- \left[\underbrace{V(t_0, FS) - D(t_0, FS)}_{=0}\right] \frac{dt_0}{dFS}$$

The terms in brackets in Eq. 19 are equal to 0, since $V(t, FS) = D(t, FS)$ at $t = t_0$ and $t = t_1$. Therefore the integral is the only term which remains. The second derivative is shown in Eq. 20, as a result of Leibniz integral rule:

$$\underbrace{\frac{d^2\tau}{dFS^2}}_{>0} = \int_{t_0}^{t_1} \underbrace{\frac{\partial^2 V(t,FS)}{\partial FS^2}}_{0} - \underbrace{\frac{\partial^2 D(t,FS)}{\partial FS^2}}_{\leq 0} dt + \left[\underbrace{\frac{\partial V(t_1,FS)}{\partial FS} - \frac{\partial D(t_1,FS)}{\partial FS}}_{<0}\right] \underbrace{\frac{dt_1}{dFS}}_{<0} - \left[\underbrace{\frac{\partial V(t_0,FS)}{\partial FS} - \frac{\partial D(t_0,FS)}{\partial FS}}_{\geq 0}\right] \underbrace{\frac{dt_0}{dFS}}_{\geq 0} \quad \text{Eq. 20}$$

To prove the second derivative is positive ($\frac{\partial^2 \tau}{\partial FS^2} > 0$), three steps are taken:

Step I: Show that $\frac{\partial^2 V(t,FS)}{\partial FS^2} = 0 \; \forall \; t_0 \leq t \leq t_1$

This is true by the problem statement, since $V(t, FS)$ is decreased proportionally to FS at all t.

Step II: Show that $\frac{\partial^2 D(t,FS)}{\partial FS^2} \leq 0 \; \forall \; t_0 \leq t \leq t_1$

We start by presenting an expression for the extrapolated value of a departure curve $D^E(t_0^O, FS)$ at t_0^O after a shift of FS. Note that $D^E(t, FS) = D(t, FS) \; \forall \; t \in [t_0, t_1]$. The expression is given in Eq. 21 and $D^E(t, FS)$ is depicted in

Figure 20, which is a close-up of cumulative plot with curves displayed for only two values for FS. Note that without loss of generality we assume that $t_0^O = 0$, $V(t_0^O, FS^O) = 0$, as can be seen in Figure 20 and that $FS^O = 0$. Therefore, the first term in Eq. 21 is equal to $D^E(t_0, FS) - D^E(0,0)$ as shown in Figure 20 and the second term is equal to $D(t_0, FS) - D^E(0, FS)$.

$$D^E(0,FS) = V(t_0,FS) - \mu \times t_0 = \int_0^{t_0} \frac{\partial V(t,FS)}{\partial t} dt - \mu \times t_0 \quad \text{Eq. 21}$$

Figure 20. Cumulative plot focused on initial delay times t_0

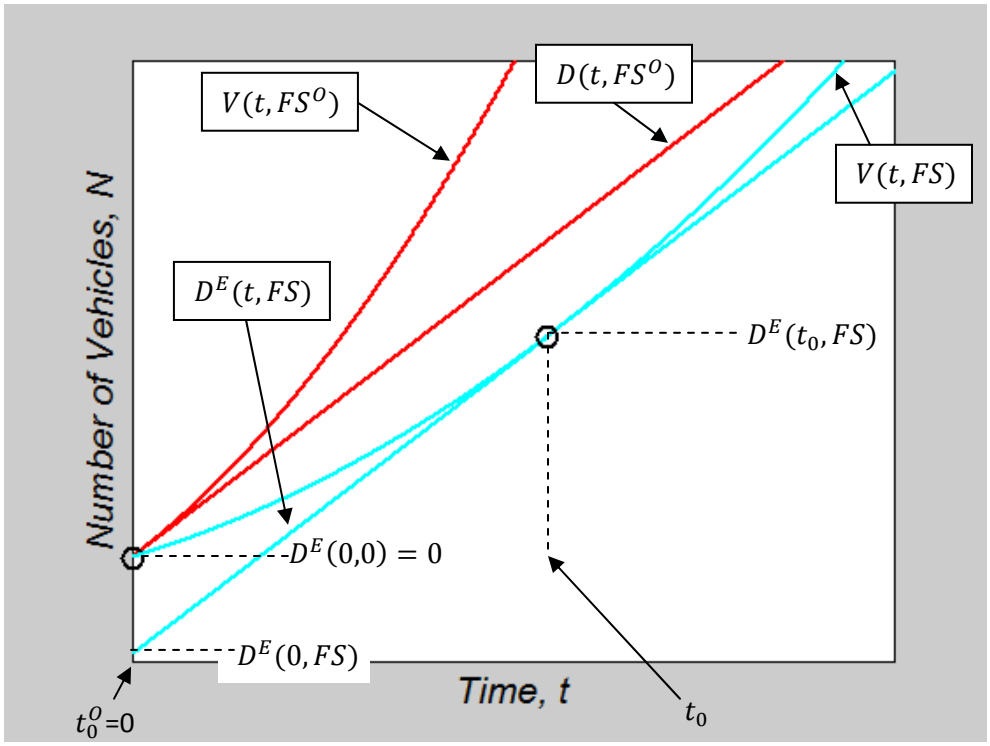

Although Eq. 21 only provides $D^E(0,FS)$, the derivatives of this value with respect to FS are in fact equal to those of $D^E(t,FS)\ \forall\ t$. This follows from the assumption of constant departure rate ($\mu = \frac{\partial D(t,FS)}{\partial t}$), since $\frac{\partial^2 D}{\partial t \partial FS} = 0\ \forall\ t$. Therefore $\frac{\partial^2 D^E(0,FS)}{\partial FS^2} \leq 0 \Rightarrow \frac{\partial^2 D(t,FS)}{\partial FS^2} \leq 0\ \forall\ t$, so we can simply prove $\frac{\partial^2 D^E(0,FS)}{\partial FS^2} \leq 0$.

Using Leibniz rule, the first derivative of Eq. 21 is shown in Eq. 22. The integral in Eq. 22 is non-positive, given our problem statement that increasing FS causes a proportional decrease in $V(t,FS)\ \forall\ t$. The latter terms are equal and therefore cancel one another, since $\frac{\partial V(t_0,FS)}{\partial t} = \frac{\partial D(t_0,FS)}{\partial t} = \mu$.

$$\underbrace{\frac{dD(0,FS)}{dFS}}_{\leq 0} = \underbrace{\frac{dD^E(0,FS)}{dFS}}_{\leq 0} = \partial\left[\int_0^{t_0} \frac{\partial V(t,FS)}{\partial t} dt\right] \Big/ \partial FS - \mu \times \frac{dt_0}{dFS} \qquad \text{Eq. 22}$$

$$= \underbrace{\int_0^{t_0} \frac{\partial^2 V(t,FS)}{\partial t \partial FS} dt}_{\leq 0} + \underbrace{\frac{\partial V(t_0,FS)}{\partial t}\frac{dt_0}{dFS} - \mu \times \frac{dt_0}{dFS}}_{0}$$

The second derivative is shown in Eq. 23. The signs of the terms are obvious due to the problem statement.

$$\underbrace{\frac{d^2D(0,FS)}{dFS^2}}_{\leq 0} = \underbrace{\frac{d^2D^E(0,FS)}{dFS^2}}_{\leq 0} = \int_0^{t_0} \underbrace{\frac{\partial^3 V(t,FS)}{\partial t \partial FS^2}}_{0} dt + \underbrace{\frac{\partial^2 V(t_0,FS)}{\partial t \partial FS}}_{\leq 0}\underbrace{\frac{dt_0}{dFS}}_{\geq 0} \qquad \text{Eq. 23}$$

Step III. Next the second and third terms of Eq. 20 are considered. Based on Figure 19 and Figure 20 one can easily intuit the signs of these terms as shown in Eq. 20. Therefore we must finally show that the magnitude of the second term exceeds the third as shown in Eq. 24. This will be done by showing that $|A| > C$ and $|B| > D$.

$$\overbrace{\left[\underbrace{\frac{\partial V(t_1,FS)}{\partial FS} - \frac{\partial D(t_1,FS)}{\partial FS}}_{<0}\right]}^{A}\overbrace{\underbrace{\frac{dt_1}{dFS}}_{<0}}^{B} > \overbrace{\left[\underbrace{\frac{\partial V(t_0,FS)}{\partial FS} - \frac{\partial D(t_0,FS)}{\partial FS}}_{\geq 0}\right]}^{C}\overbrace{\underbrace{\frac{dt_0}{dFS}}_{\geq 0}}^{D} \qquad \text{Eq. 24}$$

First we show that $|A| > C$ in Eq. 24. This is easily verified if we assume, without loss of generality, a shifting coordinate system, such that $t_0 = 0$, and $V(t_0, FS) = 0$ for any given FS. Note that this assumption fits within all those in the problem statement. Using the shifting coordinates provides an intuitive argument which is shorter than an explicit derivation. The idea of shifting coordinates is again used in section 3.4. The concept could have also been used to show step II of this proof, however the formulas of that step will be referred to in section 3.4. Under the assumption of shifting coordinates we know that Eq. 25 holds for all FS. The first and second inequalities are in accordance with Eq. 22, since

$\int_0^{t_0} \frac{\partial^2 V(t,FS)}{\partial t \partial FS} dt = \int_0^0 \frac{\partial^2 V(t,FS)}{\partial t \partial FS} dt = 0$. The third equality is a result of the problem statement, which tells us that $V(0, FS) = 0 \; \forall \; FS$.

$$0 = \frac{\partial D(t_1, FS)}{\partial FS} = \frac{\partial D(t_0, FS)}{\partial FS} = \frac{\partial V(t_0, FS)}{\partial FS} \qquad \text{Eq. 25}$$

Therefore we are left to consider only $\frac{\partial V(t_1,FS)}{\partial FS} < 0$ in Eq. 24, for which the sign is obvious. As a result $|A| > C$.

Finally we show that $|B| > D$. Again we assume, without loss of generality, the same shifting coordinate system. Therefore $\frac{dt_1}{dFS} < 0$ and $\frac{dt_0}{dFS} = 0$, which are a result of with $\frac{\partial V(t_1,FS)}{\partial FS} < 0$ and $\frac{\partial V(t_0,FS)}{\partial FS} = 0$, respectively.

Therefore through the three steps we have proven that

$$\frac{d^2\tau}{dFS^2} > 0 \Rightarrow \frac{\partial^2 W}{\partial FS^2} > 0 \Rightarrow \frac{\partial^2 W_T}{\partial FS^2} > 0 \qquad \blacksquare$$

This implies that $\frac{\partial^2 Conc^M}{\partial FS^2} > 0 \; \Rightarrow \; \frac{\partial^2 Conc^{MN}}{\partial FS^2} > 0$ under the assumption of linearly increasing $Conc^N$ with respect to FS, and in turn there exists the potential for a three-regime isopleth diagram to occur as shown in Figure 13. Note that in the situation that increasing FS entirely eliminates queuing, then $\frac{\partial^2 Conc}{\partial FS^2} = 0$ for higher values of FS, which still allows for the existence of Regime T.

The proof can additionally be adapted for the case of a two-peaked congested period, which represents a situation in which a queue is present throughout the day between morning and evening commutes. This is depicted in Figure 16.

Figure 21. Two-peaked congested period

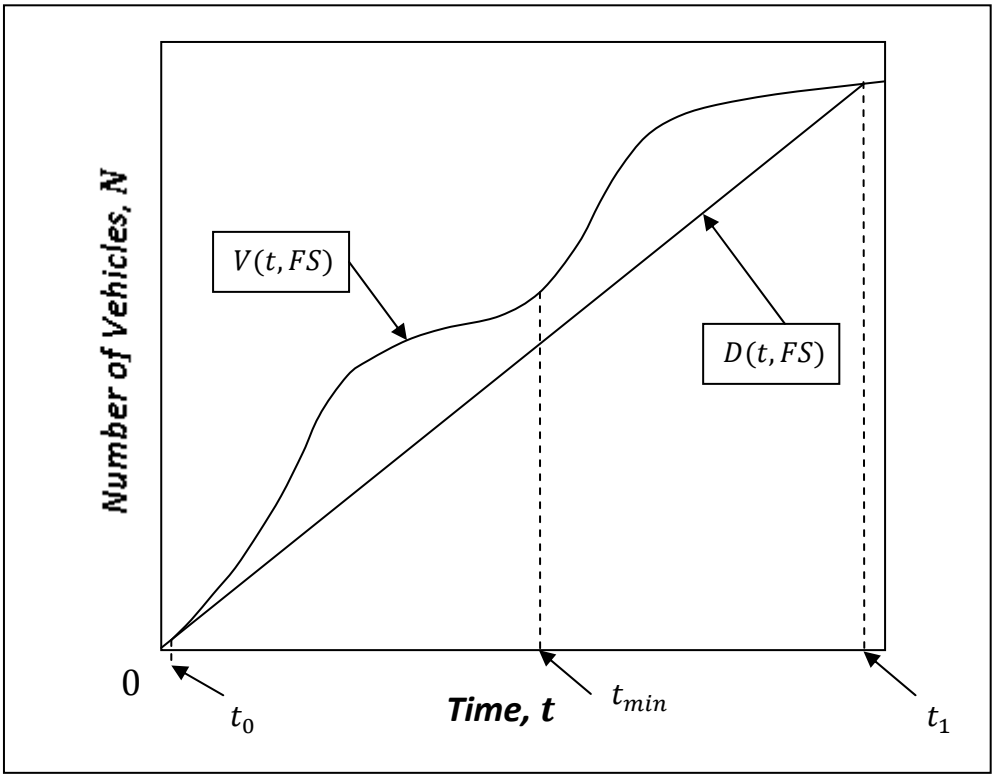

Eq. 26 shows $\frac{d^2\tau}{dFS^2}$ for the two-peaked case. The signs can be intuited similarly to those in Eq. 20 and the third term can be shown to be larger than the fourth by using similar logic to step III in the proof. The only caveat is that as FS is increased, $V(t, FS)$ may become less than $D(t, FS)$ for t between the peaks, in which case $\frac{d^2\tau}{dFS^2}$ maintains a positive sign as a result of the proof being applicable to each peak period separately.

$$\underbrace{\frac{d^2\tau}{dFS^2}}_{>0} = \int_{t_0}^{t_{min}} \underbrace{\frac{\partial^2 V(t,FS)}{\partial FS^2}}_{0} - \underbrace{\frac{\partial^2 D(t,FS)}{\partial FS^2}}_{\leq 0} dt + \int_{t_{min}}^{t_1} \underbrace{\frac{\partial^2 V(t,FS)}{\partial FS^2}}_{0} - \underbrace{\frac{\partial^2 D(t,FS)}{\partial FS^2}}_{\leq 0} dt$$
$$+ \left[\underbrace{\frac{\partial V(t_1,FS)}{\partial FS} - \frac{\partial D(t_1,FS)}{\partial FS}}_{<0}\right] \underbrace{\frac{dt_1}{dFS}}_{<0} - \left[\underbrace{\frac{\partial V(t_0,FS)}{\partial FS} - \frac{\partial D(t_0,FS)}{\partial FS}}_{\geq 0}\right] \underbrace{\frac{dt_0}{dFS}}_{\geq 0} \quad \text{Eq. 26}$$

3.4. Additional Traffic Considerations

In this section the analysis of section 3.3 is extended with further traffic considerations. Table 3 provides a list of variables introduced in section 3.4.

Table 3. Variables introduced in section 3.4

$c(t_W, t_A)$	Total individual cost
$c_S(c(t))$	Individual schedule cost
$c_W(c(t))$	Individual wait cost
$Conc$	$PM_{2.5}$ Concentration
n	Vehicle accumulation
P	Travel production
t_A	Actual time of arrival for individual
t_{max}	Time of maximum queue length
t_W	Desired time of arrival for individual
V_X	Virtual arrival curve for vehicle type X

The first traffic consideration of note is that the freight vehicle virtual arrival curve $V_T(t, FS)$ is likely to be inverted versus that for passenger vehicles $V_C(t, FS)$, as shown in Figure 17. This is consistent with data which indicate that freight operators generally avoid having trips during passenger commuting periods (Dreher and Harley, 1998; Vilain and Wolfrom, 2000). Nevertheless the total virtual arrival curve (i.e. $V(t, FS) = V_T(t, FS) + V_C(t, FS)$) is still likely to be S-shaped, since passenger vehicles generally comprise the majority of traffic flow (Grenzeback et al., 1990) and since latent demand would form

(Small, 1992). Therefore one can expect that $\frac{d^2\tau}{dFS^2}$ is increased further in addition to the base case in section 3.3, for relatively low FS. This can be understood through Eq. 27 which is the result of plugging Eq. 22 into Eq. 19.

$$\frac{d\tau}{dFS} = \int_{t_0}^{t_1} \frac{\partial V(t,FS)}{\partial FS}\,dt - \int_{t_0}^{t_1}\int_{0}^{t_0} \frac{\partial V^2(t,FS)}{\partial t \partial FS}\,dt\,dt \qquad \text{Eq. 27}$$

Again, we use the concept of moving coordinates such that t_0=0 and $V(t_0, FS)$=0 for any given FS. As a result, the second term in Eq. 27 is equal to 0, leaving only the first term for consideration. Based on the graphical construction shown in Figure 17, one can see that the first term is likely to be very similar for the inverted and base cases, for given values of t_0 and t_1. However, on the peripheries on the peak period, the slope of $\frac{\partial V^R(t,FS)}{\partial FS}$ is less than $\frac{\partial V(t,FS)}{\partial FS}$. As a result, $\frac{d^2\tau}{dFS^2}$ is greater, since $\frac{d^2t_0}{dFS^2}$ is less and $\frac{d^2t_1}{dFS^2}$ is greater, causing decreasing marginal reduction in the duration of the peak period. On the other hand, the opposite effect occurs towards the middle of the peak period. Therefore, the inverted virtual arrival curve increases the likelihood of the existence of Regime T.

Figure 22 - Inverted logistics vehicle trip demand

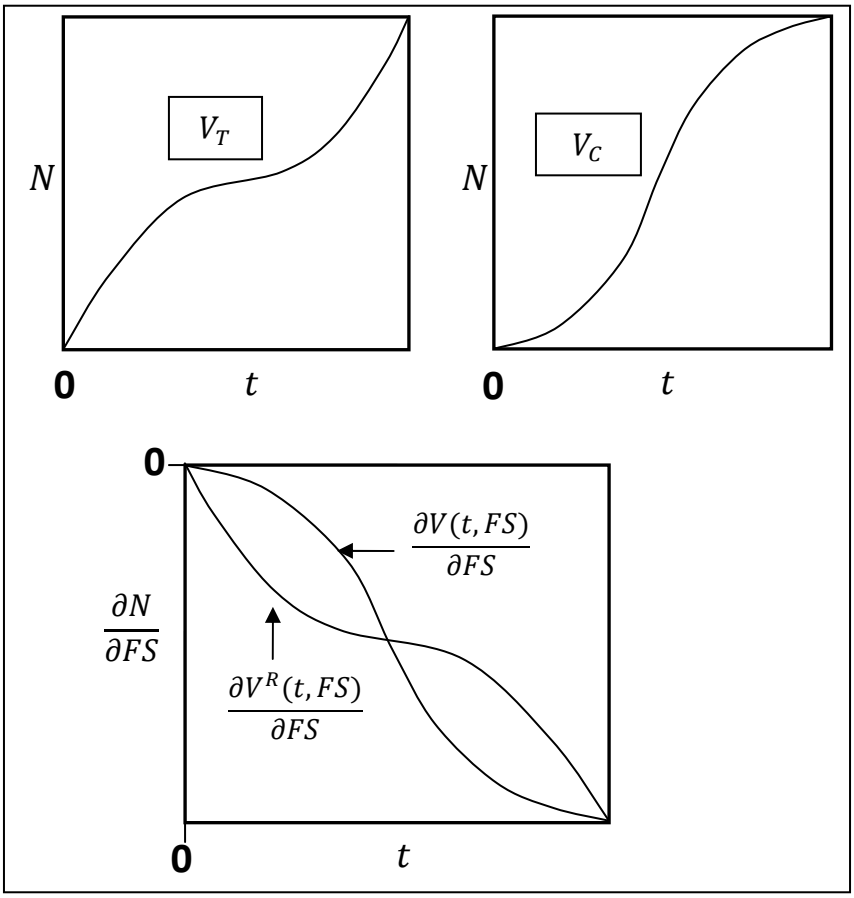

Next, the issue of schedule delay and its influence on arrival time during peak periods is discussed. The main concept, which has been the subject of multiple studies (Newell, 1987; Small, 1992), is that a reduction in trip demand during the peak causes a shift in the selected arrival time by the remaining drivers, since they do not actually arrive at their most desired time of arrival. The presentation by (Newell, 1987) will be used to develop intuition regarding the effect this may have on $\frac{d^2\tau}{dFS^2}$. The arrival time decision made by each individual is modeled as a tradeoff between schedule delay cost $c_S(t_W - t_A)$ and the cost of waiting in queued traffic $c_W(w(t_A))$, which results in Eq. 28. $c_W(w(t_A))$ is a function of the individual waiting time $w(t_A)$ and $c_S(t_W - t_A)$ is a function of the difference between the desired time of arrival t_W and the actual time of arrival at the bottleneck t_A. Eq. 29 displays the derivative of the

individual total cost with respect to t_A, thus showing that the optimal solution occurs at the time at which the two cost terms have equal derivatives, assuming differentiable cost functions. This allows for the use of the graphical construction in Figure 18.

$$c(t_W, t_A) = c_W\big(w(t_A)\big) + c_S(t_W - t_A) \qquad \text{Eq. 28}$$

$$\frac{\partial c(t_W, t_A)}{\partial t_A} = w'(t_A)c'_W(w(t_A) - c'_s(t_W - t_A) = 0 \qquad \text{Eq. 29}$$

Figure 23. The individual arrival time decision problem

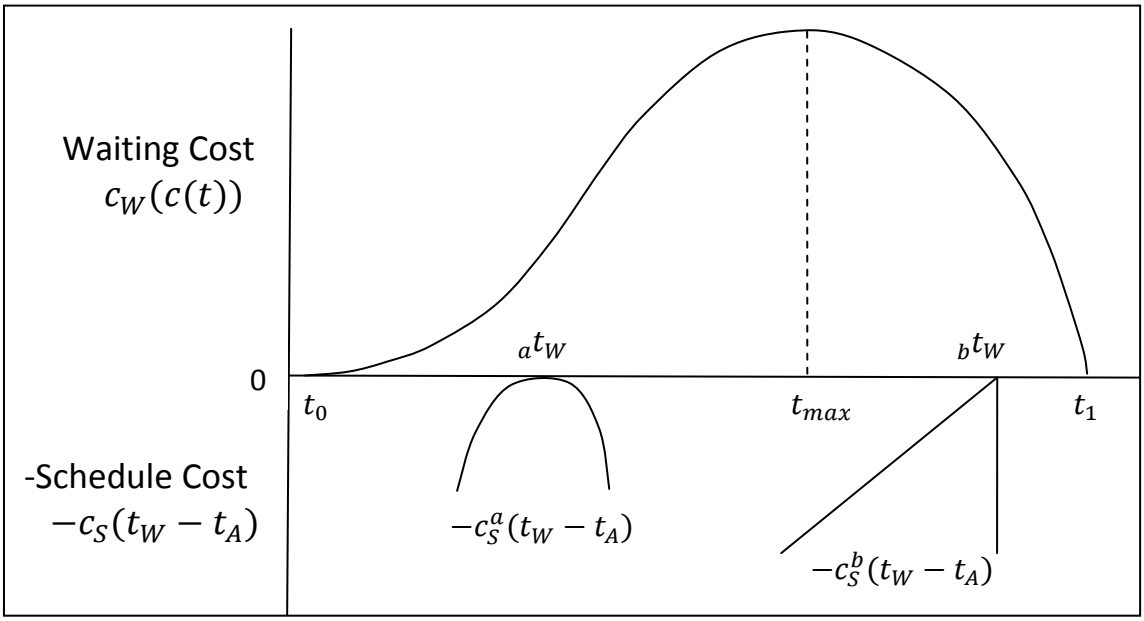

From Figure 18, one can see that the solution to the individual arrival problem can be solved by finding the point of tangency if one was to move $-c_S(t_W - t_A)$ towards $c_W\big(c(t)\big)$ unless no tangent time exists, in which case t_W is optimal. A variety of schedule cost functions are plausible, of which two examples are drawn in Figure 18.

The effects of schedule delay will be assessed by first assuming an increased FS, and subsequently a decreasing $V(t, FS)$ and $c_W\big(c(t)\big)$. Then we can examine the resulting changes in individual arrival

times in accordance with Figure 18, and the implications for $\frac{d^2\tau}{dFS^2}$. An increase in FS results in a decrease in $\partial c_W(c(t))/\partial t \; \forall \; t$ (i.e. $0 \geq \frac{\partial^2 V(t,FS)}{\partial t \partial FS} \; \forall \; t \Rightarrow 0 \geq \frac{\partial^2 c_W(c(t))}{\partial t \partial FS} \; \forall \; t$. Therefore an individual with desired arrival time t_W^a and the associated convex $c_S^a(t_W - t_A)$ shown in Figure 18, who previously arrived at $t_A < t_W^a$, would arrive later to minimize $c(t_W, t_A)$ after an increase in FS. Similarly, an individual schedule cost function shaped like $c_S^a(t_W - t_A)$, but having a desired arrival time at t_W^b, is likely to arrive later or at t_W^b after an increase in FS. On the other hand, and individual with $c_S^b(t_W - t_A)$, t_W^b, and who previously arrived $t < t_{max}$ at would simply shift her t_A towards the inflection point of $c_W(w(t))$ occurring for $t < t_{max}$.

The examples above indicate the imprecision in predicting how individuals will shift their arrival times after an increase in FS, due to variety of forms of $c_S(t_W - t_A)$ which may exist. Nevertheless it would appear that two general conclusions can still be made. The first has to do with the magnitude of the effects of schedule delay on $\frac{d\tau}{dFS}$ in comparison to the initial effects of an off-peak policy. $V(t, FS)$ can change in a variety of ways, depending on the structure of $c_S(t_W - t_A)$ for each individual. However if we assume that the distribution of forms for the individual $c_S(t_W - t_A)$ does not vary greatly across time, we can conclude that the total schedule delay effect on $V(t, FS)$ is commensurate with the magnitude of $\frac{d\tau}{dFS}$. This occurs since there are fewer drivers remaining in the queue as FS is increased, and in turn fewer making an arrival shift based on schedule delay. Therefore we can conclude that this effect is unlikely to dominate the sign of $\frac{d^2\tau}{dFS^2}$.

The second conclusion one might draw is based on empirical results that indicate a shift in arrivals towards the middle of the peak-period (Small, 1992). We can expect that there is likely to be less overall shift in arrivals towards t_{max} versus the case of reducing passenger trip demand. This is in accordance with the inverted arrival curve of Figure 17, which indicates that there is likely to be less effect on the

arrival curve nearer t_{max}. Subsequently the "level of congestion" (Small, 1992), may be more likely to improve, since drivers may be incentivized to shift their time of arrival to towards the peripheries of the peak period , when the queues would undergo greater reduction.

The concept of improving the level of congestion corresponds to improving S^M as a result of increasing FS. This is represented in traffic flow theory by an increase in μ for a link or travel production P in the case that traffic on a network can be modeled using a macroscopic fundamental diagram (MFD) (Geroliminis and Daganzo, 2008). As a result there would be less decrease for $D(t, FS)\ \forall\ t$, for a given FS . Such an improvement would result from a decrease in k for a FD or accumulation n for a MFD. We note that the implications of section 3 hold for the MFD in general, however it is introduced here, since one can expect that there exist more situations in which an off-peak policy is likely to affect the average traffic state across a network than for a single bottleneck. The concavity of the FD is well established and commonly assumed in traffic analyses (Daganzo, 2005; Gentile et al., 2005). Similarly the concavity of the MFD can be seen empirically (Geroliminis and Daganzo, 2008) and has been proven analytically (Daganzo and Geroliminis, 2008). Therefore under the reasonable assumptions that traffic is in a congested state, and that $\frac{\partial^2 k}{\partial FS^2} = 0$ and $\frac{\partial^2 n}{\partial FS^2} = 0$ for the FD and MFD respectively, we know that $\frac{\partial^2 \mu}{\partial k^2} \geq 0$ and $\frac{\partial^2 P}{\partial n^2} \geq 0$, for cases in which increasing FS improves S^M.

We can now use these intuitions in the context of the equations of section 3.3., to examine the effects on $\frac{d^2\tau}{dFS^2}$. The concavity of the FD and MFD implies a decrease for $\frac{\partial^2 V(t_0,FS)}{\partial t \partial FS}$ and an increase for $\frac{dt_0}{dFS}$, since t_0 is greater than the case in which μ does not improve, for a given FS. In turn $\frac{\partial^2 D(t,FS)}{\partial FS^2}$ is reduced according to Eq. 23. This implies an increase for $\frac{d^2\tau}{dFS^2}$, through Eq. 20. Invoking the idea of shifting coordinates we can also see that $\frac{\partial V(t_1,FS)}{\partial FS}$ and $\frac{dt_0}{dFS}$ would further decrease for a given FS, so we can interpret that the sum of the latter two terms of Eq. 20 is increased, also contributing to increasing $\frac{d^2\tau}{dFS^2}$.

Increased traffic flow reduces exhaust concentrations caused per vehicle, due to the vehicle-induced heat flux component. However, the effect of this phenomenon tends to wane for increasing flows (i.e. $\frac{\partial Conc}{\partial q}$>0, $\frac{\partial^2 Conc}{\partial q^2}$>0) (Benson, 1984), since there are decreasing marginal impacts on localized atmospheric instability with respect to q. One can reasonably expect that for cases of interest, peak-period traffic is in a congested state, whereas nighttime traffic is uncongested. Therefore in the case that FS affects μ during the peak period there would be decreasing marginal environmental benefits (i.e. $\frac{\partial^2 (Conc^M)}{\partial FS^2}$ is increased). In addition, for the uncongested off-peak there would be increasing marginal environmental damage associated with the vehicle-induced heat flux (i.e. $\frac{\partial^2 (Conc^N)}{\partial FS^2}$ is increased), under the reasonable assumption that the flow would increase approximately linearly with FS. This assumption is necessary, since $\frac{\partial Conc}{\partial FS} = \frac{\partial Conc}{\partial \mu} \times \frac{\partial \mu}{\partial FS}$ and $\frac{\partial^2 \mu}{\partial FS^2} \geq 0$ holds for the peak period in which traffic is congested due to the concavity of the FD, but not for the off-peak, uncongested conditions. Nevertheless, the assumption is justified for two reasons. The first is our assumption that that $\frac{\partial^2 k}{\partial FS^2} = 0$. And the second is because the uncongested portion of the FD is often linear with a slope defined by s_f so that $\frac{\partial^2 q}{\partial k^2} = 0$, since in this portion of the FD traffic speed is not very sensitive to k, except near k_c (Newell, 1993).

Double parking by freight vehicles making deliveries is a common cause of traffic congestion (Han et al., 2005; Yannis, 2006). Similarly to the time dependence of arrivals, this issue is highly context-dependent and therefore only a coarse discussion is provided. Double parked-vehicles can be thought to essentially reduce q by eliminating the flow in a particular lane. If several double-parked vehicles are stationed on a single link then the flow would not improve until all the parked vehicles are removed, which would imply a sudden decrease in $\frac{d^2 \tau}{dFS^2}$ for high values of FS. However if we assume that across a network there is a uniform distribution of double-parked vehicles per link and delay resulting from the loss of

flow on each link, then the improvements to q and subsequently μ can generally be thought to be linear with respect to FS. Therefore, the sign of $\frac{d^2\tau}{dFS^2}$ could generally be expected to be unaffected.

3.5. Incorporating additional environmental impacts

This section ties together other environmental issues presented in section to the isopleth diagrams and related issues presented in section 3.1 through 3.4.

The basic causes for the two-regime form of the isopleth diagrams of section 3.2 are the higher environmental impacts associated with off-peak operations and the shape of the emission factor curve provided in Figure 13. The introduction of Regime T in Figure 13 is caused by the decreasing marginal environmental benefits associated with increasing FS. Therefore, if such characteristics exist for pollutants other than particulates, the regimes of their corresponding isopleth diagrams would follow a similar form.

Five additional variables of concern potentially have similar characteristics:

1. O_3 concentrations

2. CO_2 emissions

3. Fuel Consumption

4. Logistics operator costs

5. Congestion costs to passenger-vehicle drivers

Note that CO_2 emissions, fuel consumption and costs are strongly correlated, so we will simply discuss CO_2. Both O_3 (Nazaroff and Alvarez-Cohen, 2001) and CO_2 emissions (Quak and de Koster, 2008) can increase as a result of shifts in logistics trips to midday and off-peak, respectively. In addition, Figure 24

through Figure 27 indicate that the form of the emission factor curves are similar to that in Figure 13. Therefore, there exists the potential for the two-regime isopleth diagrams to describe O_3 concentrations and CO_2 emissions. Decreasing marginal benefits are likely to occur similarly for NO_x and VOC to the case of $PM_{2.5}$, since emissions would be higher in queued traffic as shown in Figure 24 and Figure 25.

This shows that the third regime can exist for an O_3 isopleth diagram. However, it should be acknowledged that an O_3 isopleth diagram could take on two-regime and one-regime forms due to the complexities of atmospheric chemistry involved in the O_3 formation process. In addition, the importance of knowing that $\frac{\partial^2 W}{\partial FS^2} > 0$, instead of the more obvious $\frac{\partial^2 W_T}{\partial FS^2} > 0$ becomes apparent since we may account for the decreasing benefits of CO_2 emissions, including passenger vehicles. As a result, we may state that the third regime can exist for a CO_2 emissions isopleth diagram, potentially creating a significant policy concern. This shows that the third regime can exist for an O_3 isopleth diagram. However, it should be acknowledged that an O_3 isopleth diagram could take on two-regime and one-regime forms due to the complexities of atmospheric chemistry involved in the O_3 formation process. In addition, the importance of knowing that $\frac{\partial^2 W}{\partial FS^2} > 0$, instead of the more obvious $\frac{\partial^2 W_T}{\partial FS^2} > 0$ becomes apparent since we may account for the decreasing benefits of CO_2 emissions, including passenger vehicles. As a result, we may state that the third regime can exist for a CO_2 emissions isopleth diagram, potentially creating a significant policy concern.

Figure 24. E2007 Heavy-heavy duty vehicle VOC emission factors for Alameda County

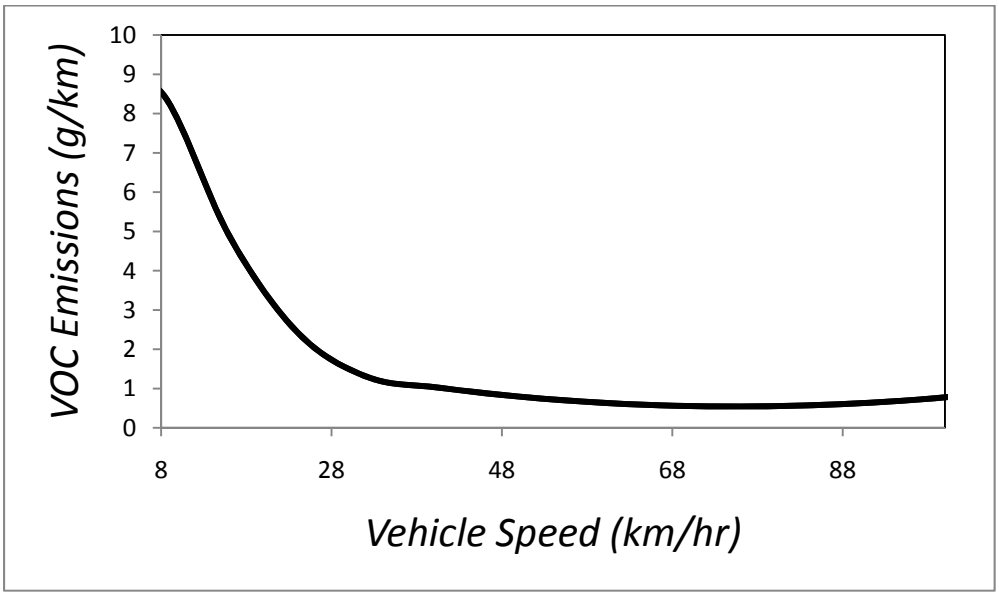

Figure 25. EMFAC2007 Heavy-heavy duty vehicle NO_x emission factors for Alameda County

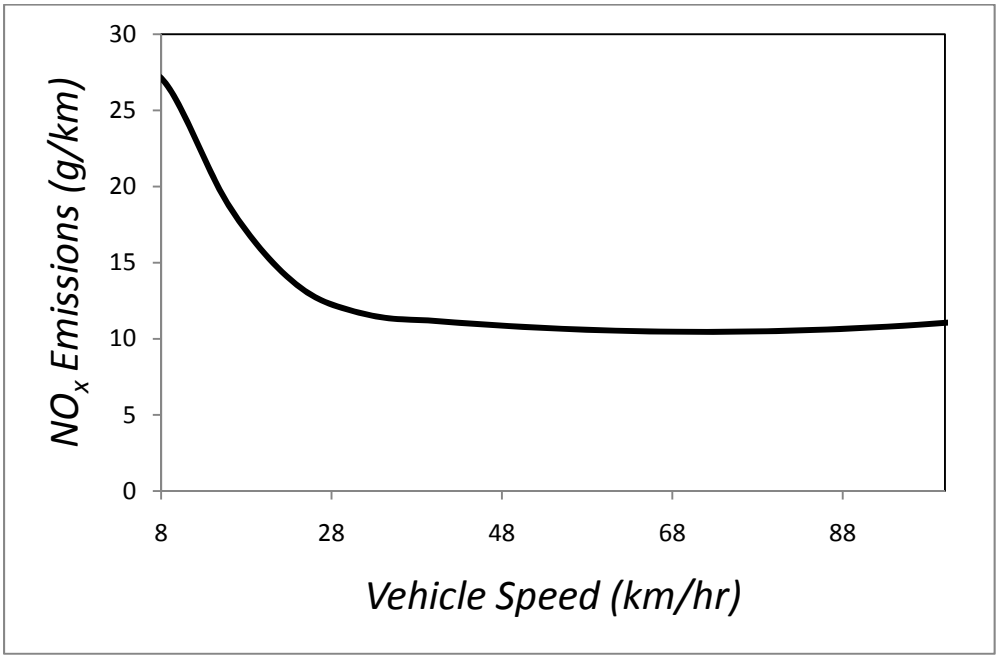

Figure 26. E2007 Heavy-heavy duty vehicle CO_2 emission factors for Alameda County

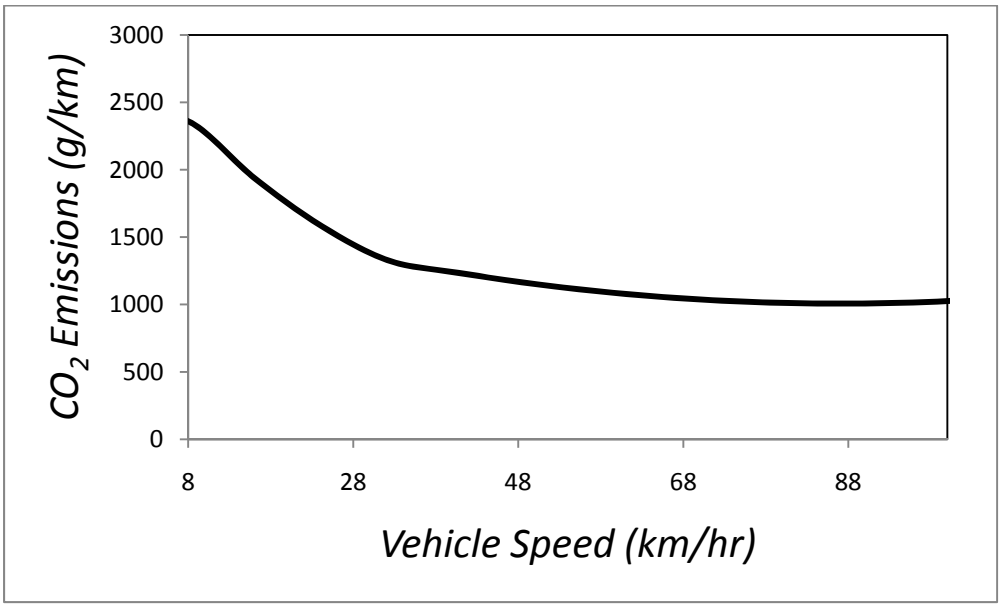

Figure 27. E2007 Passenger cars CO_2 emission factors for Alameda County

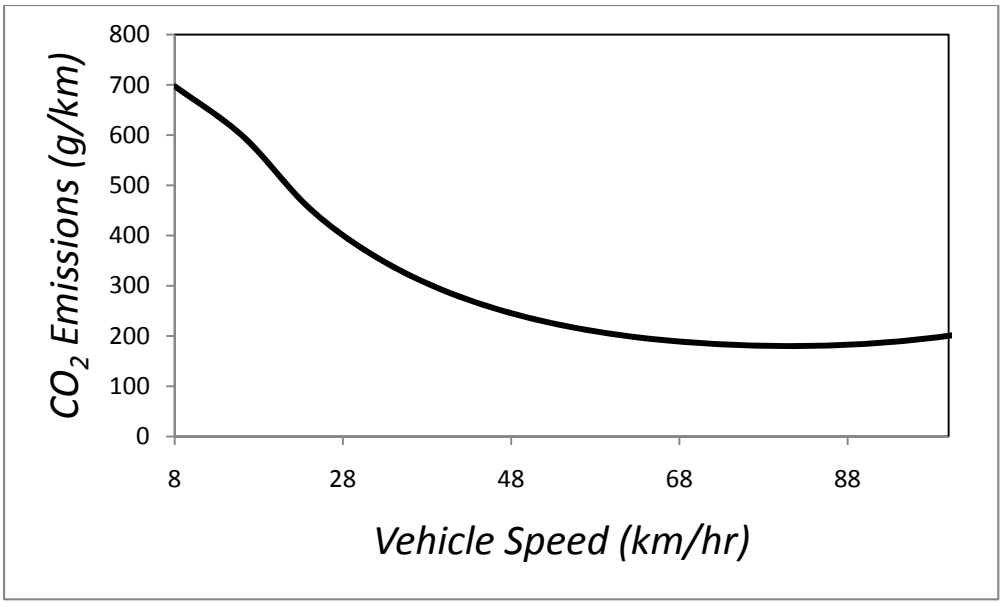

A final conclusion can be derived regarding the reduction of the environmental impacts resulting from metropolitan freight policies. The isopleth diagrams of sections 3.2 and 3.3 indicate that environmental impacts are minimal for high S^M and low FS. This is likely to be the case for CO_2 emissions as well and in some contexts for O_3 concentrations as well. In addition, if latent demand is ignored, relatively low

impacts and improved total delay for passenger traffic could be expected to result from high S^M and FS. Consequently, the most beneficial policies are likely to be those that improve traffic speeds during congested daytime hours. This provides further justification for the host of traffic control methods aimed at increasing flows to reduce total delay during congested periods (Daganzo, 2007; Daganzo et al., 2002). The single caveat of this general conclusion is that situations may exist in which a changed spatial distribution and speed in queues could cause increased exhaust concentrations in more sensitive locations.

4. Conclusion

This paper focuses on estimating the change in freight vehicle exhaust concentrations and human intake as a result of nighttime policies, indicating that increases are likely in many metropolitan settings. This calls into question the generally assumed environmental benefits of nighttime freight operations. The unintended result is shown to be more likely to occur in inland climates during the summer for California, and more generally, climates that exhibit significant diurnal variation. However, environmental benefits are likely to occur for situations with relatively low daytime traffic speeds, as shown through isopleth diagrams. Nevertheless, there exist decreasing marginal benefits associated with nighttime policies, creating situations in which such policies may initially reduce environmental impacts, but cause damage if too many trips are shifted out of the peak period. These results are depicted in isopleths diagrams, which provide a method that can be utilized in the future to more easily assess whether or not an off-peak policy is likely to cause environmental damage. In accordance with these results and the mounting environmental concerns regarding freight vehicle emissions, this paper highlights the importance of conducting comprehensive assessments of logistics policies, which account for the subtleties of both transportation and environmental systems.

Acknowledgement

This research was supported by the University of California, Berkeley's Center for Future Urban Transport (a Volvo Center of Excellence).

References

Ahrens, C. D. (2003) *Meteorology Today*. Brooks/Cole.

Banks, J. (1989) Freeway Speed-Flow-Concentration Relationships: More Evidence and Interpretations (With Discussion and Closure). *Transportation Research Record,* 1225, 53-60.

Bay Area Air Quality Management District *BAAQMD Meteorological Data*. http://www.baaqmd.gov/tec/data/#, Accessed on 11/7/2008.

Bennett, D., T. E. McKone, J. S. Evans, W. W. Nazaroff, M. D. Margni, O. Jolliet and K. R. Smith (2002) Defining Intake Fraction. *Environmental Science and Technology,* 36, 207A-211A.

Benson, P. E. (1984) *Caline4 - A Dispersion Model For Predicting Pollutant Concentrations Near Roadways*. California Department of Transportation.

Benson, P. E. (1992) A review of the development and application of the Caline3 and Caline4 models. *Atmospheric Environment,* 26B, 379-390.

Browne, M., J. Allen, S. Anderson and A. Woodburn (2006) Night-Time Delivery Restrictions: A Review. *Recent Advances in City Logistics* pp. 245-258 Elsevier.

BST Associates (2008) *PierPASS Review: Final Report*. Prepared for PierPASS Inc.

California Air Resources Board (2006) *EMFAC2007 v2.3*.

California Air Resources Board *West Oakland Study*. California Air Resources Board, http://www.arb.ca.gov/ch/communities/ra/westoakland/westoakland.htm, Accessed on 11/7/2008.

Caltrans (2008) *2007 Annual Average Daily Truck Traffic on the California State Highway System*. Traffic Data Branch.

Campbell, J. (1995) Using Small Trucks to Circumvent Large Truck Restrictions: Impacts on Truck Emissions and Performance Measures. *Transportation Research Part A,* 29, 445-458.

Dablanc, L. (2007) Goods transport in large European cities: Difficult to organize, difficult to modernize. *Transportation Research A,* 41, 280-285.

Daganzo, C. (2007) Urban gridlock: Macroscopic modeling and mitigation approaches. *Transportation Research Part B,* 41, 49-62.

Daganzo, C. F. (1995a) A Pareto Optimum Congestion Reduction Scheme. *Transportation Research B,* 29, 139-154.

Daganzo, C. F. (1995b) Properties of Link Travel Time Functions Under Dynamic Loads. *Transportation Research B,* 29, 95-98.

Daganzo, C. F. (1997) *Fundamentals of Transportation and Traffic Operations*. Pergamon.

Daganzo, C. F. (2005) A variational formulation of kinematic waves: basic theory and complex boundary conditions. *Transportation Research B,* 39, 187-196.

Daganzo, C. F. and N. Geroliminis (2008) An analytical approximation for the macroscopic fundamental diagram of urban traffic. *Transportation Research B,* 42, 771-781.

Daganzo, C. F., J. Laval and J. C. Muñoz (2002) *Ten Strategies for Freeway Congestion Mitigation with Advanced Technologies*. Calironia PATH Research Report.

Daunfeldt, S.-O., N. Rudholm and U. Ramme (2009) Congestion charges and retail revenues: Results from the Stockhom road pricing trial. *Transportation Research A,* 43, 306-309.

Dreher, D. B. and R. A. Harley (1998) A Fuel-Based Inventory for Heavy-Duty Diesel Truck Emissions. *Journal of the Air and Waste Management Association,* 48, 352-358.

Eliasson, J., L. Hultkrantz and L. Rosqvist (2009) Stockholm Congestion Charging Trial. *Transportation Research A,* 43, 237-310.

Facanha, C. and A. Horvath (2006) Environmental Assessment of Freight Transportation in the U.S. *International Journal of Life-Cycle Assessment,* 11, 229-239.

Forkert, S. and C. Eichhorn *Innovative Approaches in City Logistics: Inner-City Night Delivery*. Niches, http://www.niches-transport.org/, Accessed on 11/5/2008.

Gentile, G., L. Meschini and N. Papola (2005) Macroscopic arc performance models with capacity constraints for within-day dynamic traffic assignment. *Transportation Research B,* 39, 319-338.

Geroliminis, N. and C. Daganzo (2005) *A review of green logistics schemes used in cities around the world*. U.C. Berkeley Center for Future Urban Transport, A Volvo Center of Excellence.

Geroliminis, N. and C. F. Daganzo (2008) Existence of urban-scale macroscopic fundamental diagrams: Some experimental findings. *Transportation Research B,* 42, 759-770.

Giuliano, G. and T. O'Brien (2007) Reducing port-related truck emissions: The terminal gate appointment system at the Ports of Los Angeles and Long Beach. *Transportation Research D,* 12, 460-473.

Google (2008a) *Google Earth 4.3*.

Google *Google Maps*. http://maps.google.com/maps?hl=en&tab=wl, Accessed on 11/9/2008.

Grenzeback, L. R., W. R. Reilly, P. O. Roberts and J. R. Stowers (1990) Urban Freeway Gridlock Study: Decreasing the Effects of Large Trucks on Peak-Period Urban Freeway Congestion. *Transportation Research Record,* 1256, 16-26.

Han, L. D., S.-M. Chin, O. Franzese and H. Hwang (2005) Estimating the Impact of Pickup- and Delivery-Related Illegal Parking Activities on Traffic. *Transportation Research Record,* 1906, 49-55.

Hensher, D. A. and S. M. Puckett (2007) Congestion and variable user charging as an effective travel demand management instrument. *Transportation Research A,* 41, 615-626.

Holguin-Veras, J. (2008) Necessary conditions for off-hour deliveries and the effectiveness of urban freight road pricing and alternative financial policies in competitive markets. *Transportation Research A,* 42, 392-413.

Holguin-Veras, J. and M. Cetin (2009) Optimal tolls for multi-class traffic: Analytical formulations and policy implications. *Transportation Research A,* 43, 445-467.

Holguin-Veras, J., Q. Wang, N. Xu, K. Ozbay, M. Cetin and J. Polimeni (2006) The impacts of time of day pricing on the behavior of freight carriers in a congested urban area: Implications to road pricing. *Transportation Research A,* 40, 744-766.

Hu, S., S. Fruin, K. Kozawa, S. Mara, S. E. Paulson and A. M. Winer (2009) A wide area of air pollutant impact downwind of a freeway during pre-sunrise hours. *Atmospheric Environment,* 43, 2541-2549.

Janic, M. (2007) Modelling the full costs of an intermodal and road freight transport network. *Transportation Research D,* 12, 33-44.

Kinney, P., M. Aggarwal, M. Northridge, N. Janssen and P. Shepard (2000) Airborne Concentrations of PM2.5 and Diesel Exhaust Particeles on Harlem Sidewalks: A Community Pilot Study. *Environmental Health Perspectives,* 108, 213-218.

Lago, A. and C. F. Daganzo (2007) Spillovers, merging traffic and the morning commute. *Transportation Research B,* 41, 670-683.

Marshall, J. D. (2005) *Inhalation of Vehicle Emissions in Urban Environments*. UC Berkeley Energy and Resources Group (PhD Thesis).

Marshall, J. D., W. J. Riley, T. E. McKone and W. W. Nazaroff (2003) Intake fraction of primary pollutants: motor vehicle emissions in the South Coast Air Basin. *Atmospheric Environment,* 37, 3455-3468.

Marshall, J. D., S.-K. Teoh and W. Nazaroff (2005) Intake fraction of nonreactive vehicle emissions in U.S. urban areas. *Atmospheric Environment,* 39, 1363-1371.

McElroy, M. B. (2002) *The Atmospheric Environment: Effects of Human Activity*. Princeton University Press.

McKinnon, A. (2003) Logistics and the Environment. *Handbook of Transport and the Environment* (eds. D. A. Hensher and K. J. Button) pp. 665-685 Elsevier.

Mohan, M. and T. A. Siddiqui (1998) Analysis of various schemes for the estimation of atmospheric stability classification. *Atmospheric Environment,* 32, 3775-3781.

Nazaroff, W. and L. Alvarez-Cohen (2001) *Environmental Engineering Science*. John Wiley & Sons.

Newell, G. F. (1987) The Morning Commute for Nonidentical Travelers. *Transportation Science,* 21, 74-88.

Newell, G. F. (1993) A Simplified Theory of Kinematic Waves in Highway Traffic, Part II: Queuing at Freeway Bottlenecks. *Transportation Research B,* 27B, 289-303.

OECD (2003) *Delivering the Goods-21st Century Challenges to Urban Goods Transport*.

Olszewski, P. and L. Xie (2005) Modeling the effects of road pricing on traffic in Singapore. *Transportation Research A,* 39, 755-772.

Panis, L. I. and C. Beckx (2007) Trucks Driving at Night and Their Effect on Local Air Pollution. *Proceedings of the European Transport Conference*.

Pasquill, F. (1961) The estimation of the dispersion of windborne material. *The Meteorological Magazine,* 90, 33-49.

PeMS *Freeway Performance Measurement System (PeMS)*. University of California, Bekeley, California Partners for Advanced Transit and Highways and California Department of Transportation, https://pems.eecs.berkeley.edu/, Accessed on 11/7/2008.

Pfafflin, J. R. and E. N. Ziegler (2006) *Encyclopedia of Environmental Science and Engineering*. CRC Press.

PierPASS *PierPASS Releases Revised OffPeak Schedule at the Ports of Los Angeles and Long Beach*. http://www.pierpass.org/press_room/releases/?id=72, Accessed on 9/25/2009.

Port of Oakland *Port of Oakland Initiates Night Gates Trial Project*. http://www.portofoakland.com/newsroom/pressrel/view.asp?id=12, Accessed on 11/19/2008.

Port of Oakland *Facts & Figures*. Port of Oakland, Accessed on 11/7/2008.

Quak, H. J. and R. de Koster (2007) Exploring retailer's sensitivity to local sustainability policies. *Journal of Operations Management,* 25, 1103-1122.

Quak, H. J. and R. de Koster (2008) Delivering Goods in Urban Areas: How to Deal with Urban Policy Restrictions and the Environment. *Transportation Science, Articles in Advance. Sept. 12*, 1-17.

Quak, H. J. and R. de Koster (2009) Delivering Goods in Urban Areas: How to Deal with Urban Policy Restrictions and the Environment. *Transportation Science,* 43, 211-227.

Sathaye, N., A. Horvath and S. Madanat (2009) Unintended impacts of increased truck loads on pavement supply-chain emissions. *Transportation Research A,* Accepted for Publication.

Sathaye, N., Y. Li, A. Horvath and S. Madanat (2006) *The Environmental Impacts of Logistics Systems and Options for Mitigation*. Working Paper VWP-2006-4. U.C. Berkeley Center for Future Urban Transport, A Volvo Center of Excellence

Seinfeld, J. H. and S. N. Pandis (1997) *Atmospheric Chemistry and Physics: From Air Pollution to Climate Change*. John Wiley & Sons.

Sheffi, Y. (1985) *Urban Transportation Networks*. Prentice-Hall Inc.

Small, K. A. (1992) Trip Scheduling in Urban Transportation Analysis. *American Economic Review,* 82, 482-486.

Transport for London *Congestion Charging*. http://www.tfl.gov.uk/roadusers/congestioncharging/, Accessed on 9/25/2009.

U.S. Environmental Protection Agency (2002) *Health Assessment Document for Diesel Engine Exhaust*. National Center for Environmental Assessment, Office of Research and Development.

U.S. Environmental Protection Agency *National Ambient Air Quality Standards*. http://www.epa.gov/air/criteria.html, Accessed on 11/8/2008.

Ubillos, J. B. (2008) The costs of urban congestion: Estimation of welfare losses arising from congestion of cross-town link roads. *Transportation Research A,* 42, 1098-1108.

Verhoef, E. T. (2005) Speed-flow relations and cost functions for congested traffic Theory and empirical analysis. *Transportation Research A,* 39, 792-812.

Vickrey, W. S. (1969) Congestion theory and transport investment. *American Economic Review,* 59, 251-260.

Vilain, P. and P. Wolfrom (2000) Value Pricing and Freight Traffic: Issues and Industry Constraints in Shifting from Peak to Off-Peak Movements. *Transportation Research Record,* 1707, 64-72.

Wu, J., D. Houston, F. Lurmann, P. Ong and A. Winer (2009) Exposure of PM2.5 and EC from diesel and gasoline vehicles in communities near the Ports of Los Angeles and Long Beach, California. *Atmospheric Environment,* 43, 1962-1971.

Yannis, G., Antoniou (2006) Effects of Urban Delivery Restrictions on Traffic Movements. *Transportation Planning and Technology,* 29, 295-311.

Zhang, H. M. and Y. E. Ge (2004) Modeling variable demand equilibrium under second-best road pricing. *Transportation Research B,* 38, 733-749.